



## Deglacial and Holocene vegetation and climatic changes in the southern Central Mediterranean from a direct land–sea correlation

S. Desprat<sup>1</sup>, N. Combourieu-Nebout<sup>2</sup>, L. Essallami<sup>3</sup>, M. A. Sicre<sup>2</sup>, I. Dormoy<sup>4</sup>, O. Peyron<sup>4</sup>, G. Siani<sup>5</sup>, V. Bout Roumazeilles<sup>6</sup>, and J. L. Turon<sup>7</sup>

<sup>1</sup>EPHE, Environnements et Paléoenvironnements Océaniques et Continentaux (EPOC), UMR CNRS 5805, Université Bordeaux 1, 33405 Talence, France

<sup>2</sup>LSCE, UMR 1572 CNRS/CEA/UVSQ, 91198 Gif-sur-Yvette Cedex, France

<sup>3</sup>GEOGLOB, Sfax Faculty of Sciences, 3038 Sfax, Tunisia

<sup>4</sup>UMR 6249 Chrono-Environnement, Université de Franche-Comté, 25030 Besançon, France

<sup>5</sup>IDES, Earth Sciences Department, Université Paris XI, 91405 Orsay, France

<sup>6</sup>UMR CNRS 8217 GEOSYSTEMES, Université Lille 1, 59655 Villeneuve d'Ascq, France

<sup>7</sup>EPOC UMR CNRS 5805, Université Bordeaux 1, 33405 Talence, France

Correspondence to: S. Desprat (s.desprat@epoc.u-bordeaux1.fr)

Received: 5 November 2012 – Published in Clim. Past Discuss.: 21 November 2012

Revised: 20 February 2013 – Accepted: 1 March 2013 – Published: 20 March 2013

**Abstract.** Despite a large number of studies, the long-term and millennial to centennial-scale climatic variability in the Mediterranean region during the last deglaciation and the Holocene is still debated, including in the southern Central Mediterranean. In this paper, we present a new marine pollen sequence (core MD04-2797CQ) from the Siculo-Tunisian Strait documenting the regional vegetation and climatic changes in the southern Central Mediterranean during the last deglaciation and the Holocene.

The MD04-2797CQ marine pollen sequence shows that semi-desert plants dominated the vegetal cover in the southern Central Mediterranean between 18.2 and 12.3 ka cal BP, indicating prevailing dry conditions during the deglaciation, even during the Greenland Interstadial (GI)-1. Across the transition Greenland Stadial (GS)-1 – Holocene, Asteraceae-Poaceae steppe became dominant till 10.1 ka cal BP. This record underlines with no chronological ambiguity that even though temperatures increased, deficiency in moisture availability persisted into the early Holocene. Temperate trees and shrubs with heath underbrush or maquis expanded between 10.1 and 6.6 ka, corresponding to Sapropel 1 (S1) interval, while Mediterranean plants only developed from 6.6 ka onwards. These changes in vegetal cover show that the regional climate in southern Central Mediterranean was wetter during S1 and became drier during the mid- to late Holocene. Wet-

ter conditions during S1 were likely due to increased winter precipitation while summers remained dry. We suggest, in agreement with published modeling experiments, that the early Holocene increased melting of the Laurentide Ice Sheet in conjunction with weak winter insolation played a major role in the development of winter precipitation maxima in the Mediterranean region in controlling the strength and position of the North Atlantic storm track.

Finally, our data provide evidence for centennial-scale vegetation and climatic changes in the southern Central Mediterranean. During the wet early Holocene, alkenone-derived cooling episodes are synchronous with herbaceous composition changes that indicate muted changes in precipitation. In contrast, enhanced aridity episodes, as detected by strong reduction in trees and shrubs, are recorded during the mid- to late Holocene. We show that the impact of the Holocene cooling events on the Mediterranean hydroclimate depend on baseline climate states, i.e. insolation and ice sheet extent, shaping the response of the mid-latitude atmospheric circulation.

## 1 Introduction

The Mediterranean region has received increasing attention during the past decade, since it was identified as a major “climate change hot spot” in future climate modeling projections as a result of the global increase in greenhouse gases (Giorgi, 2006; IPCC, 2007). Sensitivity of the Mediterranean climate and ecosystems to global climate change during glacial and interglacial periods has been demonstrated by numerous paleoclimatic studies. Holocene Mediterranean records show that the long-term Holocene climatic evolution in response to orbital forcing can be described by three phases: a humid phase from the start of the Holocene to 7.0 ka cal BP, a transition phase from 7.0 to 5.5 ka and an aridification phase from 5.5 ka to the present-day (Jalut et al., 2009; Finné et al., 2011; Pérez-Obiol et al., 2011). However, Holocene environmental conditions in the Mediterranean region remain a matter for debate. Delayed forest expansion in some records suggests that dry conditions may have persisted into the Holocene for several centuries to millennia in parts of the Mediterranean region (Tzedakis, 2007; Kotthoff et al., 2008a). Davis and Brewer (2009) even hypothesized that higher early Holocene moisture availability was not related to increased precipitation but decreased temperature. The respective contribution of climate and human activities to environmental changes, the contrasting and complex information provided by different proxy records and the heterogeneity of this region contribute to the existing uncertainties on the Holocene climate evolution in the different regions of the Mediterranean (Tzedakis, 2007; Roberts et al., 2011a). This is particularly true for the southern Central Mediterranean as shown by an increasing number of lake level, pollen and speleothem records depicting contrasting signals. Some paleorecords from Sicily show wetter conditions (Sadori and Narcisi, 2001; Magny et al., 2011b; Peyron et al., 2012) while others indicate drier conditions during the early Holocene (Tinner et al., 2009; Calò et al., 2012). Note that “early Holocene” is defined here as the 11.7 to 6.5 ka interval and “mid- to late Holocene” the interval from 6.5 ka to present-day. On the southern rim of the Mediterranean Sea, peat sequences from Kroumirie (Ben Tiba and Reille, 1982; Ben Tiba, 1995; Stambouli-Essassi et al., 2007) only give partial information on the Holocene vegetation history in northern Tunisia. Hence, getting a clearer picture of the long-term climatic changes in the southern Central Mediterranean is needed and will be a crucial step towards a mechanistic understanding of the regional hydroclimatic changes in response to large-scale orbital climatic changes.

Deglacial vegetation changes in the Central Mediterranean are based on few pollen sequences mainly located in central Italy and the Adriatic Sea (Watts et al., 1996; Combourieu-Nebout et al., 1998; Magri, 1999; Magri and Sadori, 1999). These records clearly show the afforestation associated with the climatic improvement of the last deglaciation as well as the response of the Mediterranean forest to millennial cli-

matic changes. However, for Tunisia, the low temporal resolution of the available records (Ben Tiba and Reille, 1982; Brun, 1983) does not allow evaluating the impact of the deglacial abrupt climate changes.

Since the identification of abrupt changes in the North Atlantic during the Holocene (Bond et al., 1997), a number of publications have shown that such changes affected the Mediterranean Sea and borderlands (e.g. synthesis papers and references therein: Magny et al., 2007a; Fletcher and Zielhofer, 2011; Peyron et al., 2011; Roberts et al., 2011b; Sadori et al., 2011). In the Central Mediterranean, records provide evidence of increased dryness during the Holocene cooling episodes which contrasts with the increase in humidity in the European mid-latitudes, above 40° N (Magny et al., 2011b). Recently, a change in nature and tempo of centennial-scale variability during the mid-Holocene has been identified in the SW Mediterranean (Fletcher et al., 2012). However, divergent information from different proxy records and chronological uncertainties are often major limitations to our understanding of abrupt climatic changes. Key questions remain about the impact of Holocene cooling events on the Mediterranean climate and ecosystems and the processes responsible for the propagation and modulation of the North Atlantic variability into the Mediterranean region.

In this paper, we present pollen data from a marine record retrieved from the Siculo-Tunisian strait providing a regional picture of climate and vegetation changes in the southern Central Mediterranean during the last deglaciation and the Holocene. Our record based on a direct land–sea correlation will bring new insight into regional long-term trends and millennial to centennial-scale climatic changes. We compare our results with other records from Central and Western Mediterranean to show a coherent pattern between records. Finally, we discuss the potential links between the Mediterranean climate evolution and the low- and mid-latitude atmospheric circulation features in relation with insolation and ice sheet forcings.

## 2 Environmental setting and potential pollen source

Core MD04-2797CQ (36°57' N 11°40' E, 771 m water-depth) was retrieved from the Siculo-Tunisian Strait. This site is located on the Tunisian margin at ~ 50 km east off Cape Bon (north-eastern Tunisia) and at ~ 110 km off Sicily (Fig. 1). Above the core site, deep waters originate from the Eastern Mediterranean flowing westward across the Siculo-Tunisian Strait and are composed of Levantine Intermediate Water and transitional Eastern Mediterranean Water (Astraldi et al., 2002). The upper water column is occupied by the Modified Atlantic Water (MAW). This water mass is fed by the Atlantic Tunisian Current (ATC) that flows eastward along the Tunisian coast through the strait (Fig. 1) (Béranger et al., 2004). The surface ocean circulation is driven by the atmospheric circulation dominated by

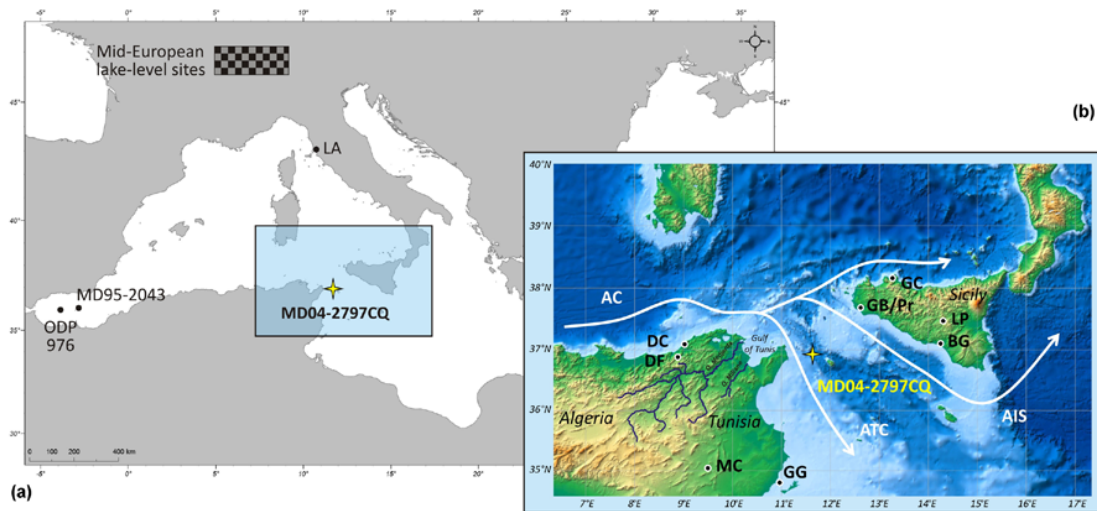


**Fig. 1.** Location of the studied core MD04-2797CQ and of other Mediterranean records mentioned in the text. **(a)** Large map: LA: Lake Accesa (Magny et al., 2007a; Finsinger et al., 2010), MD95-2043 (Fletcher and Sánchez Goñi, 2008), ODP site 976 (Combourieu-Nebout et al., 2009). Medjerda and Miliane river systems are indicated in dark blue. The mean sea surface circulation is represented by white arrows (AC: Algerian Current, ATC: Atlantic Tunisian Current, AIS: Atlantic Ionian Stream). **(b)** Inset map: sites from the southern Central Mediterranean. DF: Dar Fatma (Ben Tiba and Reille, 1982), MH: Majen Ben M’Hida (Stambouli-Essassi et al., 2007), GB/Pr: Gorgo Basso and Lake Preola (Tinner et al., 2009; Magny et al., 2011b), LP: Lake Pergusa (Sadori and Narcisi, 2001), BG: Biviera di Gela (Noti et al., 2009), MC: La Mine Cave (Genty et al., 2006), GC: Grotta di Carburangeli (Frisia et al., 2006).

westerly flow (Pinardi et al., 2005). Mean seasonal surface winds are from the NW in fall and winter and from the NW to W in spring and summer (Chronis et al., 2011).

The present-day climate in northern Tunisia is of Mediterranean-type, characterized by warm and dry summers and cool and wet winters. Orography and maritime influences modulate the climate generating meridional and zonal humidity gradients. Climate is humid to sub-humid in the northwestern mountains, semi-arid in the northeastern lowlands and arid in southern Tunisia (INRF, 1976). The autumn-winter-spring seasonal precipitation mainly derives from moisture advection from the Atlantic Ocean and western Mediterranean Sea. Summer dryness results from the development of subsidences associated with the northward displacement of the Hadley cell (Lionello et al., 2006).

Temperature and precipitation gradients and seasonality pattern control the vegetation distribution in Tunisia. The potential vegetation cover of the Medjerda watershed is dominated by *Oleo-lentiscus* maquis in the eastern semi-arid areas and by holm oak-aleppo pine (*Quercus ilex-Pinus halepensis*) forest in the southern upper semi-arid High Tell and Tunisian Dorsal. In the most north-western part of the Medjerda watershed, cork oak (*Quercus suber*) forest with *Erica arborea* underbrush and high altitude zeen oak forest (*Quercus canariensis*) prevail due to humid and sub-humid conditions in the mountains. Vegetation of Cape Bon, which is the closest landmass to our core site, is dominated by *Oleo-lentiscus* maquis, kermes oak (*Quercus coccifera*) and thuya (Gausson and Vernet, 1958; Posner, 1988; El Euch,

1995; Boussaid et al., 1999). Numerous permanent or temporary wetlands are located in Tunisia (Posner, 1988), mostly in the humid, sub-humid and upper semi-arid bioclimatic zones (INRF, 1976). Sedges are naturally dominant in the marsh zone of wetlands from northern Tunisia while halophyte plants, in particular *Chenopodiaceae*, expand in temporary wetlands from the semi-arid region (Posner, 1988).

A number of studies have shown that the marine pollen signal provides an integrated picture of the vegetation from the nearby continents (Heusser and Balsam, 1977; Naughton et al., 2007). Cores such as MD04-2797 CQ located near continental regions with well-developed hydrographic basins mainly recruit pollen from rivers (Heusser, 1978; Turon, 1984; Dupont and Wyputta, 2003). Medjerda and Miliane oueds, which are permanent water streams with watersheds covering most of northern Tunisia, provide sediments to the shelf area (Fig. 1). Wind-driven sediment input to the shelf might also be important in semi-arid regions. The mean seasonal surface winds which are northwesterly to westerly during the main pollination season (spring and summer) (Chronis et al., 2011) blow over northern Tunisia before reaching the core site. Given the large Tunisian river, the dominant winds and the surface ocean circulation, northern Tunisia is likely the main pollen source to our core site. Therefore, even though long-distance pollen transport cannot be ruled out, we interpret the pollen signal of core MD04-2797CQ as reflecting vegetation changes in this region.

### 3 Material and methods

Sediment core MD04-2797CQ was subsampled for pollen analysis every 2 to 10 cm over the first 590 cm. Samples of 1.5 to 3.5 cm<sup>3</sup> were processed using standard palynological techniques (extraction protocol available at <http://www.ephe-paleoclimat.com/ephe/Lab%20Facilities.htm>). Exotic pollen (*Lycopodium*) was added to each sample to determine pollen concentrations. After chemical and physical treatments (cold HCl, cold HF, cold KOH and sieving through 10 µm nylon mesh screens), the residue was mounted unstained in glycerol. Pollen was counted using a light microscope at 400 and 1000 (oil immersion) magnifications. A total 100 to 160 pollen grains without *Pinus* and a minimum of 20 taxa were counted in each sample; 8 out of 94 samples analysed, most of them located in the upper 80 cm, were considered as sterile due to extremely low pollen concentration. Pollen percentages for each taxon are based on the main pollen sum, excluding *Pinus* because of its over-representation in marine deposits (Heusser and Balsam, 1977; Turon, 1984). *Pinus* percentages were calculated from the main pollen sum including *Pinus*. Spores and aquatic pollen percentages were obtained from the total sum that includes all pollen grains plus aquatic plant, indeterminable pollen grains and Pteridophyta spores.

Quantitative climatic reconstructions based on the modern analogue technique (MAT) have been performed from the pollen dataset by considering the relative proportion of the different taxa in each pollen spectrum (Guiot, 1990). The methods and results for MAT application to our data are presented separately in Peyron et al. (2013). We show in the present paper synthesized results of the annual, winter and summer temperatures (TANN, MTWA, MTCO) and precipitation (Pann, Psum, Pwin) estimations.

Direct land–sea correlation is obtained in comparing pollen to marine proxies from MD04-2797CQ sediments. Dinocyst and planktic foraminifera assemblages and derived SSTs, planktic foraminifera  $\delta^{18}\text{O}$  and SST obtained from the C<sub>37</sub> alkenone unsaturation index have been published earlier (Essallami et al., 2007; Rouis-Zargouni et al., 2010). In this paper, we compare our pollen data with the new high resolution alkenone-derived SST record (Sicre et al., 2013).

## 4 Results and interpretations

### 4.1 Chronological framework and pollen analysis results

Core MD04-2797CQ chronology was established from 13 radiocarbon dates, among which 6 are from the upper 4 m of the core corresponding to the Holocene interval (Table 1). Except for the date at 0 cm, all radiocarbon dates have been replicated, thus increasing the reliability of the age–depth model. Averages of the <sup>14</sup>C date duplicates were corrected

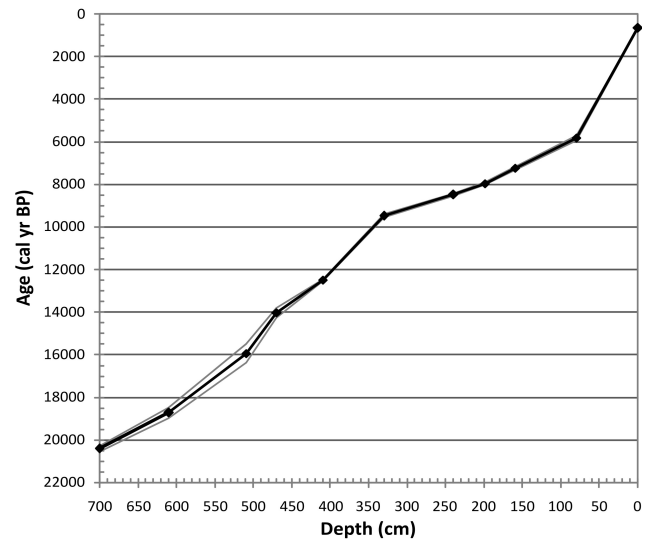


Fig. 2. Age–depth model for core MD04-2797CQ. Grey lines indicate the 1 $\sigma$  error envelope.

for a reservoir age of 400 yr for the Holocene, GS-1 and LGM intervals, of 560 yr for GI-1 (level 470 cm) and of 800 yr for Heinrich Stadial 1 (HS1) (level 510 cm), according to Siani et al. (2001). Corrected dates were calibrated using the calibration curve INTCAL 09 (Reimer et al., 2009). The age–depth model was obtained using linear interpolation between dated levels (Fig. 2). The upper 80 cm represents the last 5800 yr and is only chronologically constrained by two radiocarbon dates (5830 and 670 yr cal BP). A strong change in sedimentation rate occurred in between the two dated levels, increasing age uncertainties for this interval. Hereafter, ka and kyr will be used for ages in cal BP.

According to the age–depth model (Fig. 2), the MD04-2797CQ pollen record encompasses the last 18.2 kyr. Pollen analyses were performed at high temporal resolution (less than 100 yr) for the Holocene interval between 12.3 and 5.5 ka. Unfortunately, low pollen richness and sedimentation rate did not allow a high resolution study of the upper 80 cm. The alkenone-SST record also displays the highest temporal resolution (20 to 75 yr) over the first half of the Holocene (Sicre et al., 2013).

Pollen zones (PZ) were identified visually from the pollen diagram shown in Fig. 3 and confirmed using constrained hierarchical clustering analysis based on Euclidean distance between samples using *chclust* function from the R package *Rioja* (Juggins, 2009). Clusters were determined from pollen data filtered at 1% taxa presence in at least 5% of the samples using the R package *PaleoMas* Correa-Metrio et al., 2011). A summary of the pollen diagram description is presented in Table 2.

**Table 1.** Radiocarbon ages, corrected ages for age reservoir according to Siani et al. (2001) and calibrated ages using INTCAL 09 (Reimer et al., 2009).

| Depth (cm) | $^{14}\text{C}$ age (year BP) | Depth (cm) | Mean $^{14}\text{C}$ age from paired duplicates (year BP) | $1\sigma$ error (year) | Reservoir corrected $^{14}\text{C}$ age (year BP) | Lower cal age (year) | Upper cal age (year) | Calibrated ages (year cal BP) | $1\sigma$ error (year) |
|------------|-------------------------------|------------|-----------------------------------------------------------|------------------------|---------------------------------------------------|----------------------|----------------------|-------------------------------|------------------------|
| 0          | 1105 ± 20                     |            |                                                           | 20                     | 705                                               | 660                  | 675                  | 670                           | 10                     |
| 80         | 5425 ± 30                     | 80         | 5493                                                      | 95                     | 5093                                              | 5730                 | 5930                 | 5830                          | 140                    |
| 80         | 5560 ± 25                     |            |                                                           |                        |                                                   |                      |                      |                               |                        |
| 160        | 6760 ± 30                     | 160        | 6700                                                      | 85                     | 6300                                              | 7130                 | 7330                 | 7240                          | 120                    |
| 160.5      | 6640 ± 30                     |            |                                                           |                        |                                                   |                      |                      |                               |                        |
| 199        | 7580 ± 30                     | 199        | 7523                                                      | 81                     | 7123                                              | 7920                 | 8020                 | 7970                          | 70                     |
| 199.5      | 7465 ± 30                     |            |                                                           |                        |                                                   |                      |                      |                               |                        |
| 239.5      | 8170 ± 40                     | 240        | 8113                                                      | 81                     | 7713                                              | 8420                 | 8560                 | 8490                          | 100                    |
| 240        | 8055 ± 35                     |            |                                                           |                        |                                                   |                      |                      |                               |                        |
| 329.5      | 8810 ± 35                     | 330        | 8888                                                      | 110                    | 8488                                              | 9400                 | 9560                 | 9480                          | 110                    |
| 330        | 8965 ± 30                     |            |                                                           |                        |                                                   |                      |                      |                               |                        |
| 410        | 10 885 ± 40                   | 410        | 10 863                                                    | 32                     | 10 463                                            | 12 460               | 12 530               | 12 490                        | 50                     |
| 410.5      | 10 840 ± 40                   |            |                                                           |                        |                                                   |                      |                      |                               |                        |
| 469.5      | 12 850 ± 50                   | 470        | 12 728                                                    | 173                    | 12 168                                            | 13 790               | 14 250               | 14 020                        | 330                    |
| 470        | 12 605 ± 40                   |            |                                                           |                        |                                                   |                      |                      |                               |                        |
| 510.5      | 14 000 ± 60                   | 510        | 13 900                                                    | 141                    | 13 100                                            | 15 500               | 16 370               | 15 930                        | 620                    |
| 511        | 13 800 ± 100                  |            |                                                           |                        |                                                   |                      |                      |                               |                        |
| 610        | 15 590 ± 50                   | 610        | 15 590                                                    | 50                     | 15 190                                            | 18 460               | 18 990               | 18 730                        | 370                    |
| 610.5      | 16 160 ± 60                   |            |                                                           |                        |                                                   |                      |                      |                               |                        |
| 700        | 18 180 ± 60                   | 700        | 17 660                                                    | 70                     | 17 260                                            | 20 290               | 20 540               | 20 410                        | 180                    |
| 700        | 17 660 ± 70                   |            |                                                           |                        |                                                   |                      |                      |                               |                        |
| 939.5      | 23 300 ± 100                  | 940        | 23 415                                                    | 163                    | 23 015                                            | 27 650               | 28 110               | 27 880                        | 330                    |
| 940.5      | 23 530 ± 120                  |            |                                                           |                        |                                                   |                      |                      |                               |                        |
| 1029.5     | 26 100 ± 130                  | 1030       | 26 095                                                    | 7                      | 25 695                                            | 30 380               | 30 600               | 30 490                        | 160                    |
| 1030       | 26 090 ± 150                  |            |                                                           |                        |                                                   |                      |                      |                               |                        |

#### 4.2 Deglacial vegetation and climatic changes

Core MD04-2797CQ pollen record shows that a steppe with semi-desert plants (*Artemisia*, *Ephedra distachya*, *Ephedra fragilis*, *Chenopodiaceae*) dominates the vegetal cover up to 12.3 ka, indicating prevailing dry conditions during the last deglaciation (PZ-1-2-3; Figs. 3 and 4). Such arid environments likely characterized most of Tunisia during this period, from at least 34° N (Brun, 1985) to the northern Tunisian coast (this work). However, the moister mountainous NW part of Tunisia provided a favourable habitat for an open oak forest and a conifer forest of pine-cedar-fir in the highest altitudinal vegetation belts (Ben Tiba and Reille, 1982; Stambouli-Essassi et al., 2007).

Our marine pollen record also depicts millennial-scale vegetation changes in the southern Central Mediterranean. Two intervals of maximal semi-desert plant expansion, coeval with cold SSTs occurred between 18.2 and 14.7 ka (PZ-1) and 13.1 and 12.3 ka (PZ-3) (Figs. 3 and 4) broadly at the time of Heinrich Stadial 1 (HS1) and Greenland Stadial-1 (GS-1), respectively. Apparent age offsets between PZ-3 and GS-1 boundaries are likely related to uncertainties on

radiocarbon dating correction for reservoir age and calibration. HS1 and GS-1 are major abrupt climatic changes interrupting the last deglaciation that are widely documented as strong cooling in the North Atlantic, Europe and over Greenland (Johnsen et al., 1992; Walker, 1995; Bard et al., 2000; Peterson et al., 2000; Naughton et al., 2007). These events presumably result from the abrupt reduction in Atlantic Meridional Overturning Circulation (AMOC) due to massive iceberg discharges or freshwater releases in the North Atlantic (MacAyeal, 1993; Bond and Lotti, 1995; McManus et al., 2004; Broecker, 2006). Our sequence indicates that in southern Central Mediterranean, climate shifted toward cold and dry conditions in response to HS1 and GS-1 (Fig. 4). Prevailing arid conditions in Tunisia during GS-1 are confirmed by large aeolian terrigenous supply as detected by high illite, palygorskite and zirconium contents in our core (Bout-Roumazelles et al., 2013). Similar climatic variations were reported from Western Mediterranean marine pollen and SST records (Cacho et al., 2001; Fletcher and Sánchez Goñi, 2008; Combourieu-Nebout et al., 2009). Despite the extremely arid stadial conditions, our record indicates that deciduous tree populations, mainly deciduous

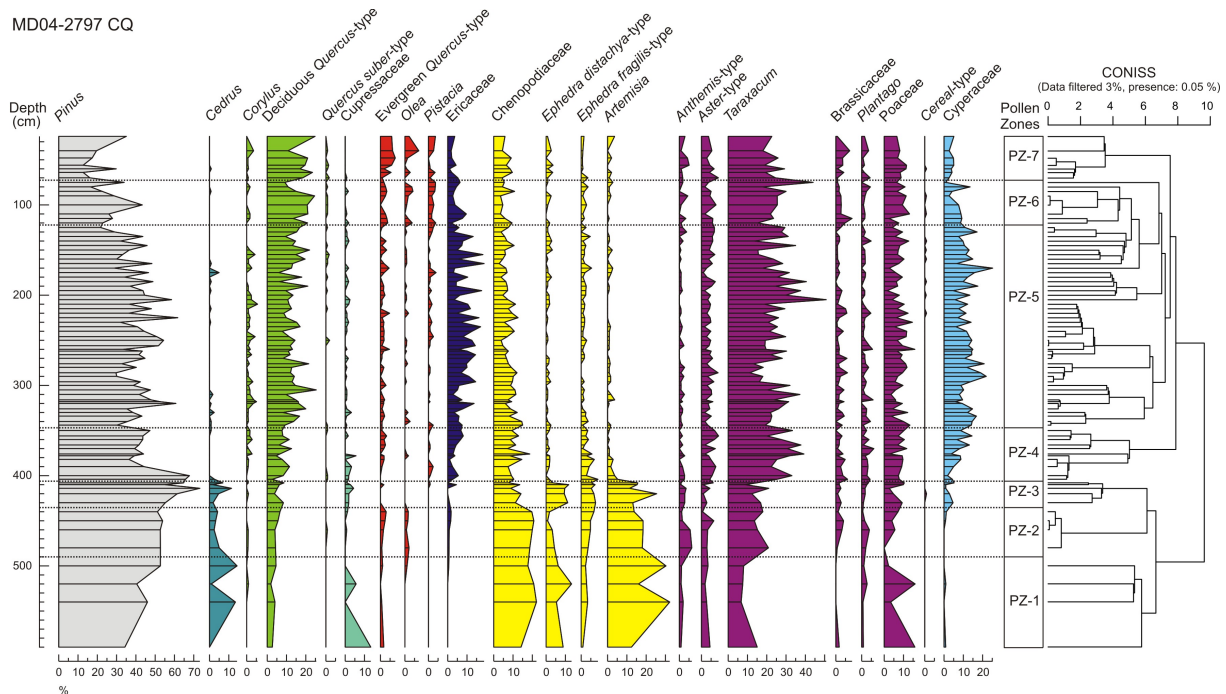


**Fig. 3.** Percentages of major pollen taxa versus depth, core MD04-2797CQ, Siculo-Tunisian Strait. Boundaries of pollen zones are based on visual inspection of data and application of clustering analysis (see text for details).

*Quercus*, probably persisted in some remaining humid areas, and that the conifers *Cedrus* and *Pinus* were present in the regional vegetation. Some deciduous taxa pollen grains may originate from Sicily or even from southern Italy where scattered woodlands have been detected (Magri and Sadori, 1999; Allen et al., 2002). However, most of the tree pollen grains recovered at our site during HS1 and GS-1 were likely transported by wind or river from NW Tunisian open oak and conifer forests located uplands during the last deglaciation (Ben Tiba and Reille, 1982; Stambouli-Essassi et al., 2007). Note the increase in *Cedrus* abundances during both stadials while deciduous oak values decrease (Fig. 3). A similar pattern has been described in marine pollen records from the Alboran Sea documenting cedar variations in the Moroccan Rif (Fletcher and Sánchez Goñi, 2008; Combourieu-Nebout et al., 2009). As discussed in Fletcher and Sanchez Goñi (2008), increases in cedar pollen abundances could reflect either (1) enhanced wind-driven pollen supply due to wind strengthening and opening of the vegetation or (2) maintenance of some degree of moisture since cedar is generally considered as a cold-tolerant, moisture-demanding conifer. Colder conditions and moisture availability at mid- to high altitudes during HS1 and GS-1 could have favoured cedar expansion at the expense of deciduous oak in NW Africa, from the Moroccan Rif to the High Tell. The Mediterranean region presents a wide range of habitats due to highly variable topography and local climate conditions which enables refugia zones during the last glacial period (Médail and Di-

adema, 2009). This work supports the idea that deciduous and conifer tree populations were maintained in the mountainous region of North Africa even during the most severe episodes of the last deglaciation.

During Greenland Interstadial-1 (GI-1), SSTs increased, semi-desert plants and cedar reduced while some deciduous and evergreen oak woodlands and Mediterranean shrubs (*Olea*) developed (PZ-2; Fig. 4). This finding is indicative of relatively warmer and wetter climatic conditions than during HS1 and GS-1. Despite the temperature rise, the semi-desert plants remained dominant and tree and shrubs expansion was limited compared to terrestrial pollen records from Italy (Magri and Sadori, 1999; Allen et al., 2002) or western Mediterranean Sea pollen records (Fletcher and Sánchez Goñi, 2008; Combourieu-Nebout et al., 2009). This result can be explained by lower water availability in the semi-arid areas of southern Central Mediterranean. Terrigenous supply to the Siculo-Tunisian Strait remained characterized by a high content of aeolian-driven particles, such as illite and palygorskite, which also indicate prevailing dry conditions during GI-1 (Bout-Roumazelles et al., 2013). Strikingly, our pollen data do not indicate a tree and shrub expansion maximum at the beginning of the GI-1 but rather slightly higher values at the end of the interstadial at ~13.4 ka following a long HS1 to GI-1 transition. This feature contrasts with the sharp temperature rise and early GI-1 optimum in Greenland ice cores (NGRIP members, 2004) (Fig. 4), and has already been identified from speleothem records from northern

**Table 2.** Description of the MD04-2797CQ pollen record.

| Pollen Zones | Interval (cm) | Pollen zone age (cal yr BP) | Description of pollen zones                                                                                                                                                                                                                                                                                                                                           | Vegetation changes                                                                                                           | Inferred climatic changes                                                           |
|--------------|---------------|-----------------------------|-----------------------------------------------------------------------------------------------------------------------------------------------------------------------------------------------------------------------------------------------------------------------------------------------------------------------------------------------------------------------|------------------------------------------------------------------------------------------------------------------------------|-------------------------------------------------------------------------------------|
| PZ-7         | 70–24         | 5300–2200                   | Highest values of evergreen <i>Quercus</i> and from 40 cm, <i>Olea</i> and low percentages of Cyperaceae and Ericaceae.<br>Peaks in deciduous <i>Quercus</i> of 20–25 %                                                                                                                                                                                               | Open Mediterranean forest with increased Mediterranean plants contribution                                                   | Decreased humidity                                                                  |
| PZ-6         | 120–75        | 6600–5300                   | Decreasing values of Cyperaceae and Ericaceae<br>Increasing percentages of Mediterranean taxa (evergreen <i>Quercus</i> , <i>Olea</i> and <i>Pistacia</i> ) and deciduous <i>Quercus</i>                                                                                                                                                                              | Expansion of an open Mediterranean forest with Asteraceae-Poaceae steppe                                                     | Transition to a period with less rainfalls                                          |
| PZ-5         | 344–125       | 10 100–6600                 | Increase in AP percentages although AP representation is weak, mainly deciduous <i>Quercus</i> and occurrences of Mediterranean taxa (evergreen <i>Quercus</i> , <i>Olea</i> and <i>Pistacia</i> )<br>High <i>Taraxacum</i> -type percentages.<br>Highest values of Ericaceae and Cyperaceae.<br>Recurrent oscillations in Cyperaceae percentages.                    | Open oak forest with heath underbrush or maquis and Asteraceae-Poaceae-Cyperaceae steppe                                     | Increased humidity<br>Centennial oscillations                                       |
| PZ-4         | 404–350       | 12 300–10 100               | Fall of semi-desert taxa percentages and rise of <i>Taraxacum</i> -type. Decreasing trend in semi-desert percentages (25 to 10 %, mainly <i>Ephedra fragilis</i> -type and Chenopodiaceae).<br>Decrease in <i>Pinus</i> and virtual absence of <i>Cedrus</i> .<br>Minor increase in deciduous <i>Quercus</i> .<br>Gradual increase of Ericaceae and Cyperaceae values | Steppe with Asteraceae, Poaceae and some semi-desert plants and development of oak woodlands with heath underbrush or maquis | Warmer conditions and gradual increase in humidity, although limited precipitations |
| PZ-3         | 430–408       | 13 100–12 300               | Rise in <i>Artemisia</i> , <i>Ephedra distachya</i> -type, <i>Cedrus</i> and Cupressaceae values                                                                                                                                                                                                                                                                      | Steppe with ragweed, chenopods, <i>Ephedra</i> and scarce cypress lowland<br>Cedar-pine conifer forest upland                | Cold and dry                                                                        |
| PZ-2         | 480–440       | 14 700–13 100               | Decrease in <i>Artemisia</i> , <i>Ephedra distachya</i> -type although semi-desert plant remains dominant, <i>Cedrus</i> and Cupressaceae values<br>Small but significant increase in AP taxa, in particular Mediterranean tree taxa (evergreen <i>Quercus</i> and <i>Olea</i> ), and Ericaceae<br>Increase in <i>Taraxacum</i>                                       | Steppe with semi-desert plants and scarce Mediterranean woodlands<br>Pine conifer forest upland                              | Warmer and less dry (limitation in water availability, decreasing trend).           |
| PZ-1         | 590–500       | 18 200–14 700               | Dominance of NAP taxa, in particular semi-desert taxa ( <i>Artemisia</i> , Chenopodiaceae, <i>Ephedra distachya</i> -type, <i>Ephedra fragilis</i> -type)<br>Continuous presence of deciduous <i>Quercus</i><br>High <i>Pinus</i> percentages and peaks of <i>Cedrus</i> and Cupressaceae                                                                             | Steppe with ragweed, chenopods, <i>Ephedra</i> and scarce cypress lowland<br>Cedar-pine conifer forest upland                | Cold and dry                                                                        |

Tunisia, southern France and southern Germany (Genty et al., 2006) as well as from pollen records from the Alboran Sea and Southern Alps (Combourieu-Nebout et al., 2009; Finsinger et al., 2011). This contrast between the high and middle latitudes may be linked to the North Atlantic oceanic and atmospheric circulations and sea ice cover (von Grafenstein et al., 1999; Genty et al., 2006). In the Southern Alps, the gradual expansion of *Quercus* have been attributed to increasing summer temperatures and longer growing season probably related to insolation (Finsinger et al., 2011). Stacked temperature records over the latitudinal bands 30–0° S and 0–30° N (Shakun et al., 2012) indicate lower temperature during GI-1 than during the Holocene and display the same peculiar increasing temperatures over the course of the interstadial. Tropical ocean temperature and associated evaporation regulate the atmospheric moisture content feed-

ing the North Atlantic storm track (Braconnot et al., 2007). Therefore, increasing inland moisture availability toward the end of GI-1 may also be associated with deglacial tropical climate changes.

### 4.3 Holocene long-term vegetation and climate changes

#### 4.3.1 Vegetation and climate in and off Tunisia

In core MD04-2797CQ, the GS-1 – Holocene transition is marked at 12.3 ka by a sharp decrease in semi-desert plants while alkenone-SSTs and summer SSTs derived from planktonic foraminifera assemblages increased by 9 °C (Essallami et al., 2007) (PZ-4; Figs. 3 and 4). As mentioned above, the apparent earlier changes in our record marking the Holocene onset may be related to our age–depth model uncertainties.

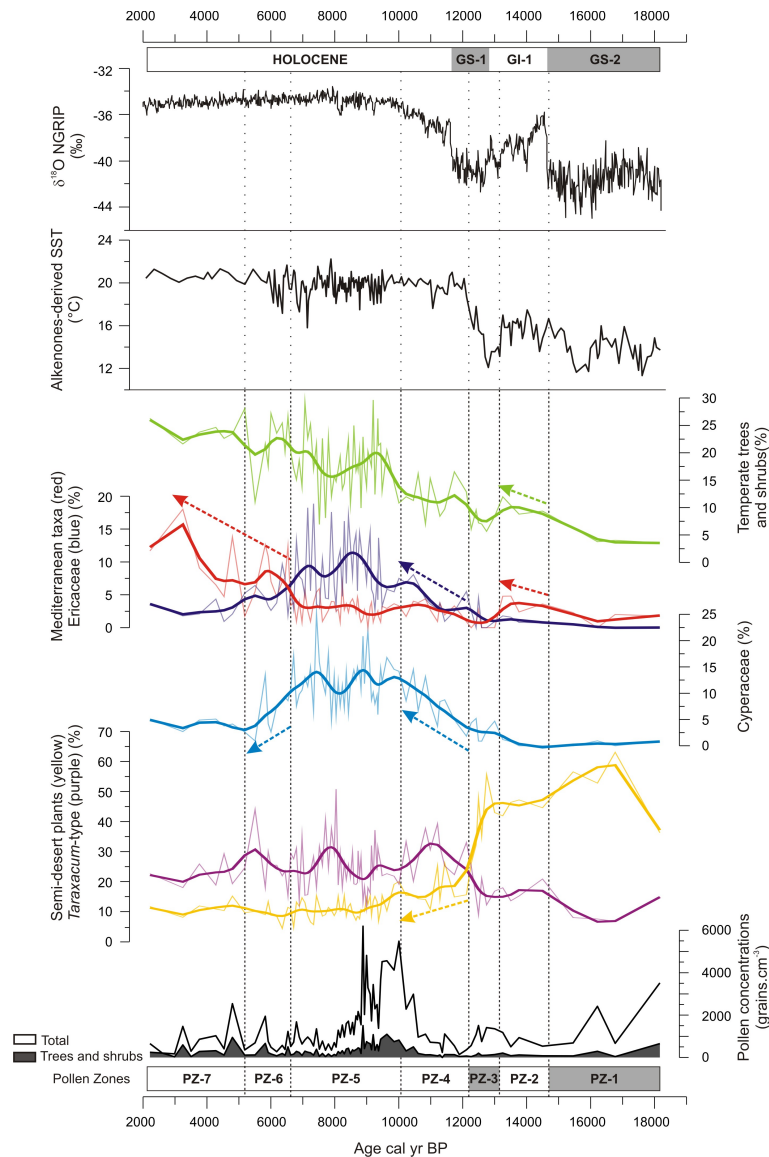


**Fig. 4.** Vegetation and climatic changes over the last 18 000 yr. From the bottom to the top: tree (excluding *Pinus*) and shrub (grey) and total (white) pollen concentrations, pollen percentages of selected pollen taxa and ecological groups, SST derived from alkenones (Sicre et al., 2013) from core MD04-2797CQ,  $\delta^{18}\text{O}$  from NGRIP ice core on GICC05 time-scale (converted to BP) (Rasmussen et al., 2006; Vinther et al., 2006). Long-term Holocene vegetation evolution has been detected by applying a smoothing cubic spline method to selected pollen taxa data. Pollen zones (bottom) and stratigraphical framework (top) are indicated. Note that we will name the Younger Dryas as Greenland Stadial 1 (GS-1), following the INITIMATE recommendations (Lowe et al., 2008), but we will keep using Heinrich Stadial (HS1) in the text (as defined by Sánchez Goñi and Harrison, 2010) because the isotopic changes during GS-2 are difficult to reconcile from one Greenland ice core to another (Rasmussen et al., 2008) and the correlation between GS-2a and HS1 has to be confirmed.

Open vegetation with Asteraceae, Poaceae and some semi-desert plants (mainly Chenopodiaceae and *Ephedra fragilis*-type) remained dominant until 10.1 ka when the open oak forest expanded. Although Mediterranean and temperate trees and shrubs slightly increased at 12.3 ka, they remained restricted at some woodlands/scrubs despite high alkenone-SSTs (Fig. 4). This vegetation change indicates a shift to warmer conditions and increased humidity during the early

Holocene but moisture availability remained too weak before 10.1 ka to enable a forest development. In the southern Mediterranean, temperature influences forest composition but moisture availability is overall critical for forest development (Quezel, 2002). During this interval, decreasing semi-desert plants and increasing Cyperaceae and Ericaceae values suggest a gradual increase in moisture availability (Fig. 4). Therefore, the abrupt tree and shrub expansion

observed at 10.1 ka would likely result from crossing ecological thresholds during gradual climatic change. The gradual decrease in aridity before 10.1 ka is supported by mineralogical and geochemical data found at core site MD04-2797CQ (Bout-Roumzeilles et al., 2013).

From 10.1 to 6.6 ka, open deciduous oak forest with heath understorey and maquis developed along with a maximal sedge expansion (PZ-5). Mediterranean plants (mainly *Pistacia*, evergreen *Quercus* and *Olea*) remained limited over this interval and only start expanding after 6.6 ka at the expense of heath maquis (PZ-6). At present-day, in the Central Mediterranean and in particular in Tunisia, Ericaceae are mainly represented by *Erica arborea*, *E. scoparia* and *E. multiflora* (Posner, 1988; Ojeda et al., 1998). Although *E. arborea* and *E. scoparia* have a wide range of distribution, they have affinities to humid climates and particularly atmospheric humid conditions (Jalut et al., 2000). This is well illustrated by the Ericaceae distribution in northern Tunisia. Both species are widely distributed in the sub-humid zones of NW Tunisia and Cape Bon in the understorey of *Quercus canariensis* and *Quercus suber* or as maquis of heather, while *E. multiflora* mainly grows in the *Olea-lentiscus* maquis or with aleppo pine and holm oak forest in the semi-arid areas of northern Tunisia (Posner, 1988). Therefore, the development of Ericaceae along with deciduous trees suggests that the most humid conditions of the Holocene occurred during this phase. Another line of evidence supporting this interpretation is the concurrent maximal development of sedges. Cyperaceae is a family comprising numerous species that can grow under a wide range of ecological conditions, although most of them develop in humid areas (Brun, 1985). Therefore, increased precipitation can potentially favour their contribution in the Asteraceae-Poaceae steppe. Sedge expansion can also reflect enhanced humid habitats, such as inland or coastal wetlands that are common features in northern Tunisia. For instance, extensive sedge marshland surrounded Garaet el Ichkeul Lake until dam constructions dramatically decreased water supply (Ramdani et al., 2001). Part of the strong sedge representation in our record might also result from coastal environment modifications related to post-glacial sea-level rise up to 6.6 ka. The highest sedge percentages are also seen in MD95-2043 and ODP 976 sites during the same period, although lower than in our sequence. In these Alboran Sea records, sedges are associated with maximum forest development sustained by the most humid conditions of the Holocene (Fletcher and Sánchez Goñi, 2008; Combourieu-Nebout et al., 2009). Our pollen record therefore suggests that the 10.1–6.6 ka interval is the wettest Holocene phase. However, water availability was probably not high enough to sustain a closed forest development in northern Tunisia. Decreasing Ericaceae and Cyperaceae between 6.6 and 5.3 ka (PZ-6) suggest a transition toward drier conditions. After 5.3 ka, the expansion of Mediterranean plants such as evergreen *Quercus* and *Olea* suggests lower available summer moisture and warmer winter.

Interpretation of our pollen record may appear contradictory regarding the gradual increase of temperate trees and shrubs throughout the Holocene. Changes in post-glacial sea level may have influenced our marine pollen signal by modifying the dominant pollen transport agent from fluvial to aeolian. Mediterranean post-glacial sea-level reconstructions suggest that Cape Bon coastline and Medjerda River mouth were closer to our core site until 6.8 ka when the Laurentide Ice Sheet (LIS) melting was completed (Lambeck et al., 2004). This could have led to enhance the representation of lowland relative to upland vegetation up to the end of the deglacial sea level rise and that of the upland open forest afterwards. A shift to drier climate could also have promoted aeolian transport. Although pollen transport changes may have modified the pollen signal, they do not alter the main vegetation changes. In particular, changes in the lowland shrub communities such as the replacement of heath maquis by *oleo-lentiscus* scrubs remain reliable to evaluate the main traits of the Holocene vegetation and climate history. Sedimentological analyses of core MD04-2797CQ agree with our interpretation of the pollen record. High sedimentation rates, decrease of aeolian-driven clay particles (palygorskite and illite), enhanced contribution of smectite likely reflecting fluvial supply and higher Zr/Al ratio indicate increased sediment supply to the shelf. Higher riverine discharge are likely sustained by more precipitation between 6 and 9.5 ka (Bout-Roumzeilles et al., 2013).

Precipitation estimates derived from our pollen record support the interpretation of highest rainfall between 10.1 and 6.6 ka, occurring mainly in winter, with mean annual precipitation of  $\sim 670$  kamm (Fig. 5, Peyron et al., 2013). This period coincides with the highest pollen concentrations (Fig. 4) possibly due to both strong terrigenous inputs and increased biomass. After 5.3 ka, while dryness increased on land, the SSTs show a moderate warming. This is confirmed by increased abundances of warm water dinocysts (Rouis-Zargouni et al., 2010).

#### 4.3.2 Climatic or human-induced vegetation changes

The respective role of climatic change and anthropogenic pressure since the Neolithic has been a long-standing debate in our understanding of the Mediterranean vegetation changes recorded by pollen sequences (De Beaulieu et al., 2005; Jalut et al., 2009). In Sicily, human impact appears to be detected in paleorecords since the Bronze Age and not since the Neolithic (Sadori and Giardini, 2007), and intense land use began with the Greek and Roman periods (Tinner et al., 2009). Human impact on the Tunisian environments became noticeable from the Phoenician and Carthaginian epochs (from XIIth to IIth century BC) with a strong agricultural development essentially based on cereal cultivations (Brun, 1983). However, our pollen record does not show this cereal signal. It is known that the dispersal of the large sized cereal pollen grains is poor (Vuorela, 1973), making

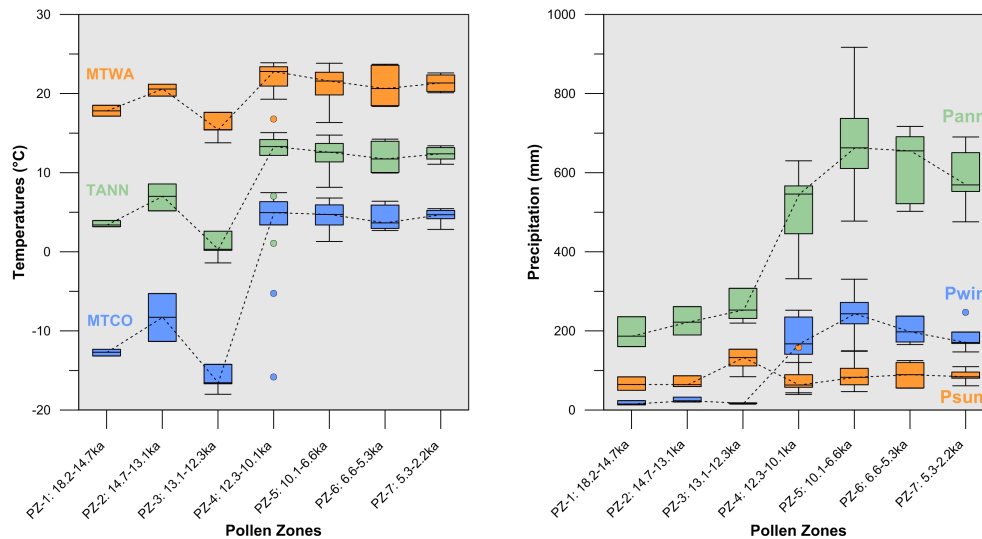


**Fig. 5.** Box-Whisker plots of estimated annual, summer and winter temperatures (TANN, MTWA, MTCO) and precipitation (Pann, Psum, Pwin) derived from the pollen data of core MD04-2797CQ (Peyron et al., 2013).

difficult to get a reliable representation of cultivated Poaceae in marine pollen records. Late Holocene *Olea* expansion is clearly detected in our record during the Bronze Age, at around 3.2 ka. However, this *Olea* increase may also have occurred during Roman times because our sequence is not well chronologically constrained between 600 and 5800 yr BP. Bronze Age or Roman olive tree expansions are also detected in Adriatic, Italian and Sicilian sequences and may result from human activities (Sadori and Narcisi, 2001; Di Rita and Magri, 2009; Combourieu-Nebout, 2012). Management of olive tree populations for fruit production started as early as the Bronze Age in the Western Mediterranean while intensive olive tree cultivation has been developed by Romans for fruits and oil in the Mediterranean region (Terral et al., 2004). However, as shown by our record, the expansion of *Olea* in southern Italy is accompanied by a widespread increase of other Mediterranean trees and shrubs that may thus reveal a concomitant vegetation response to climate (Di Rita and Magri, 2009). Therefore, although human influence cannot be discarded since the Bronze Age, beforehand, our pollen record primarily reflects climatic conditions.

#### 4.3.3 Major climatic changes in the southern Central Mediterranean

Land–sea correlation from core MD04-2797CQ indicates without chronological ambiguity that tree population expansion in southern Central Mediterranean lagged the Holocene temperature increase by approximately two millennia. Dryness in Sicily before 10.1 ka is supported by lake level and pollen data (Fig. 6g, h, i) (Sadori and Narcisi, 2001; Tinner et al., 2009; Magny et al., 2011b). Close examination of the Tunisian pollen records from Kroumirie (Stambouli-Essassi et al., 2007) and from Gulf of Gabes (Brun, 1979, 1985)

shows that the deciduous oak forest expansion in NW Tunisia and of *Olea-Pistacia* scrubs in central eastern appears delayed by at least one millennium with respect to the beginning of the Holocene (Fig. 6c). Despite loose chronological framework and temporal resolution, dry conditions at the beginning of the early Holocene appear to be a robust feature in northern Tunisian pollen records. In addition, the pollen and terrigenous records from core MD04-2797CQ parallel the  $\delta^{13}\text{C}$  signal of the Tunisian speleothem record from La Mine cave (Fig. 6d) (Genty et al., 2006). Both records suggest a gradual climatic improvement and vegetation development in southern Central Mediterranean immediately after the GS-1 cooling up to the climate optimum around 10.1 ka. This is in contrast with Lake Preola record showing an abrupt rather than gradual change in lake level (Magny et al., 2011b). This contrasting feature could be season-related with a gradual change in winter precipitation from GS-1 to 10.1 ka and an abrupt change in summer precipitation at 10.1 ka.

Increased moisture availability during the early Holocene, between 10.1 ka and 6.6 ka, is also consistent with available Tunisian and Sicilian records (Fig. 6). This accounts, for example, for the expansion of forest upland at Lake Pergusa and Majen M'Hida (Sadori and Narcisi, 2001; Stambouli-Essassi et al., 2007) and of *Pistacia* scrubs at the western Sicilian coastal sites Lake Preola and Gorgo Basso (Tinner et al., 2009; Calò et al., 2012). After 6.6 ka, our data and most of the Sicilian and northern Tunisian records show similar long-term climate changes. Pollen and sedimentary  $\delta^{18}\text{O}$  records and pollen-derived precipitation estimates from Lake Pergusa (Fig. 6h), lake level record from Lake Preola (Fig. 6i) and stalagmite record from Grotta di Carburangeli suggest a transitional period of decreasing humidity or high amplitude variability in rainfall in Sicily between the wet 10 to 7 ka

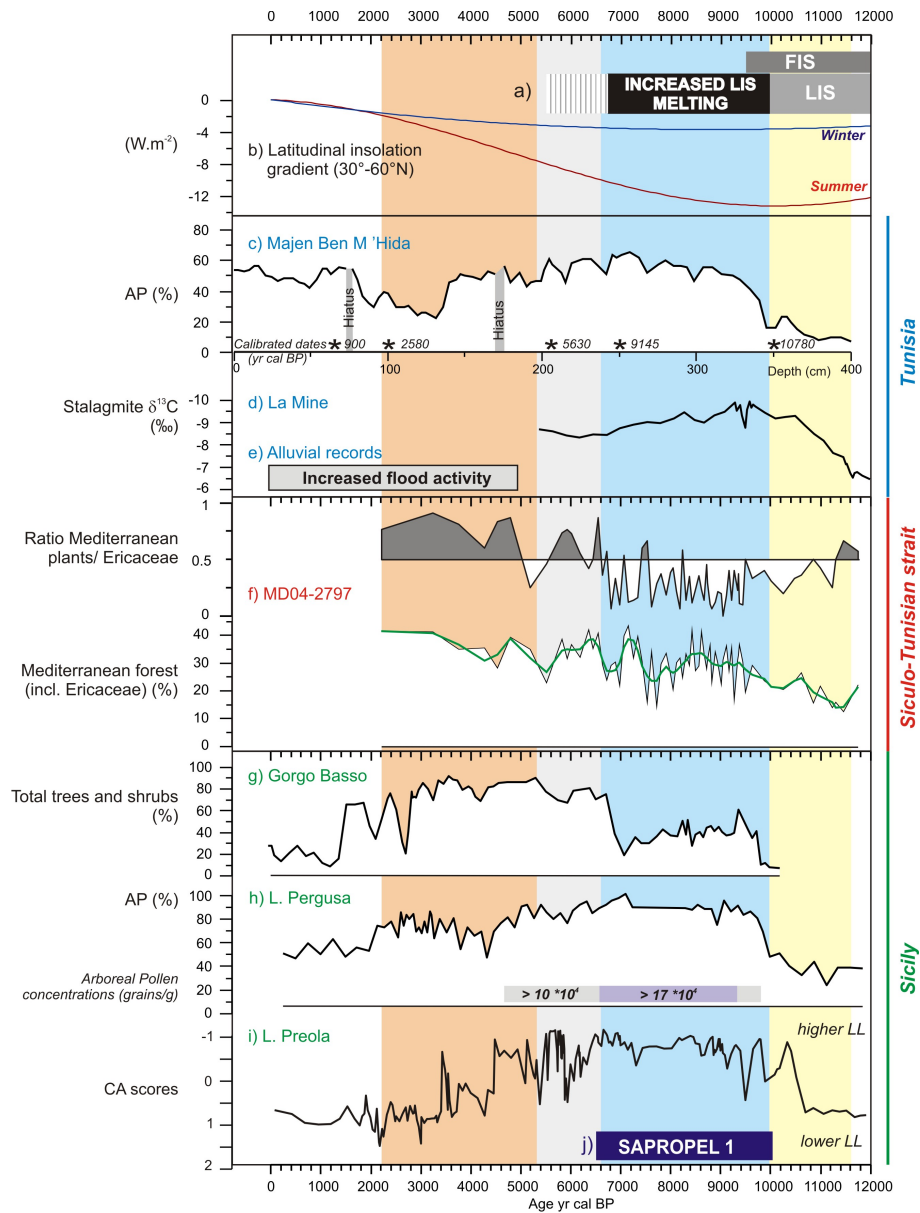


**Fig. 6.** Comparison of the pollen data from core MD04-2797CQ with other records from southern Central Mediterranean and with insolation and ice sheet forcings. *Forcings* – (a) Early Holocene ice sheet deglaciation: disappearance of the Fennoscandian Ice Sheet (FIS) at 9.5 kyr cal BP (Lundqvist and Saarnisto, 1995) and enhanced Laurentide Ice Sheet (LIS) retreat between 10 and 6.8 kyr cal BP with only small ice caps remaining up to 5.5 ka (Carlson et al., 2008); (b) Summer (JJA) and winter (DJF) latitudinal insolation gradient calculated from insolation values at 60° and 30° N (Berger and Loutre, 1991); *Tunisia* – (c) Majen Ben M'Hida peat pollen sequence: digitalized data versus depth (Stambouli-Essassi et al., 2007), asterisks: original dated levels (65 cm: 985 ± 30 yr BP; 100 cm: 2500 ± 50 yr BP; 205 cm: 4894 ± 40 yr BP; 250 cm: 8190 ± 50 yr BP; 350 cm: 9480 ± 100 yr BP) and calibrated ages using Calib 6.11 (903 (873–959); 2578 (2365–2740); 5629 (5585–5716); 9144 (9014–9287); 10 782 (10504–11143) yr cal BP); (d) δ<sup>13</sup>C speleothem record from the La Mine Cave (Genty et al., 2006); (e) Shaded bar representing the increased fluvial dynamics since 5 ka with recurrent floods associated to drier conditions, based on alluvial sequences from arid to semi-arid Central and North Tunisian floodplains (Zielhofer and Faust, 2008); *Siculo-Tunisia Strait* – (f) MD04-2797CQ pollen data: total tree and shrub percentages including Ericaceae with smoothing cubic spline (bold green line) and ratio of Mediterranean plants to Ericaceae; *Sicily* – (g) Total trees and shrubs percentages from Gorgo Basso pollen sequence (Tinner et al., 2009); (h) Arboreal pollen percentages and concentrations from Lake Pergusa sequence (Sadori and Narcisi, 2001; Sadori et al., 2011); (i) Relative changes in lake level (LL) from Lake Preola (Magny et al., 2011b); (j) Interval corresponding to Sapropele 1 after Mercone et al. (2000). The colored vertical bars represent the successive intervals as described in the text: yellow for the dry interval at the beginning of the early Holocene, blue for the wet early Holocene phase, grey for the mid-Holocene transitional interval and orange for the mid- to late Holocene phase of increasing dryness.

interval and the pronounced drier period from ca. 5–4 ka to present-day (Frisia et al., 2006; Sadori et al., 2008; Magny et al., 2011a; Peyron et al., 2012). Similarly, increasing dry conditions by ca. 5–4 ka is reflected by the replacement of the zee oak forest by a cork oak forest with heath understorey at Dar Fatma in the humid NW Tunisia (Ben Tiba and Reille, 1982). Alluvial records from the Medjerda floodplain (Fig. 6e) showing increased fluvial dynamics with recurrent floods since 5 ka also suggest prevailing arid conditions over the end of the Holocene (Zielhofer and Faust, 2008).

Pollen records from the Sicilian coastal lakes Gorgo Basso (Fig. 6g), Lake Preola and Biviera di Gela also show pronounced vegetation change ca. 7.0–6.5 ka. Conversely, this change has been interpreted as a second step of humidity increase caused by a decrease in summer dryness (Noti et al., 2009; Tinner et al., 2009; Calò et al., 2012). The climatic change inference from Biviera di Gela sequence is, however, not unequivocal. The reduction of mesophilous trees between ca. 7.0 and 5.0 ka accompanying the maximum Mediterranean forest expansion (Noti et al., 2009) may also be indicative of a rather contrasting drying trend which would be consistent with our results. Another contrasting pattern of the western Sicilian records is that no shift is recorded by 5.3 ka; the evergreen forest only declines at around 2.8–2.2 ka, likely because of intensified anthropic pressure on Mediterranean ecosystems (Tinner et al., 2009; Calò et al., 2012). A number of hypotheses, although not entirely satisfactory, have been proposed to reconcile these coastal Sicilian pollen records with Lake Preola lake-level record and Lake Pergusa pollen sequence, such as spatial heterogeneity of landscape and climate (Tinner et al., 2009) or changes in seasonal and inter-annual variability of drought (Magny et al., 2011b). Possible mis-assignment of *Pistacia* pollen taxa to the evergreen species *P. lentiscus*, while pollen grains of the evergreen and deciduous species (*P. terebinthus* and *P. atlantica*) are indistinguishable, is another plausible explanation (Sadori et al., 2011). Recently, Calò et al. (2012) also suggested that discrepancies between pollen and lake level records at the Sicilian coastal sites would come from seasonal biases of each proxy.

Rainfall seasonality in response to orbital forcing is an important issue. Lower or higher spring/summer dryness in southern Central Mediterranean between 10 and 7 ka than during the late Holocene has been deduced from continental records (Magny et al., 2011a; Calò et al., 2012), while our marine record shows that summer precipitation ( $P_{sum}$ ) at regional scale remained low (50 to 100 mm) throughout the entire Holocene with no significant change (Fig. 5; Peyron et al., 2013). However, even when  $P_{sum}$  are estimated higher, they remained < 100 mm (Magny et al., 2011a). This denotes that dry summers remained a characteristic of the Holocene climate in that region. Subtle variations in  $P_{sum}$  from semi-arid regions are particularly difficult to assess from pollen records since summer moisture availability for plants does not only depend on summer precipitation. In par-

ticular, groundwater recharge during fall and winter is critical to sustain vegetation during summer drought (Quezel, 2002; Fletcher et al., 2012). Other factors difficult to assess such as continental evaporation related to summer temperatures and cloudiness, atmospheric humidity, storminess or soil absorption/retention can be involved. In contrast, Tunisian and Sicilian pollen and speleothem records (Frisia et al., 2006; Magny et al., 2011a) agrees with our observations (Fig. 5; Peyron et al., 2013), underlying that the strongest winter and annual rainfall in the southern Central Mediterranean occurred during the 10.1–6.6 ka interval, followed by a decrease toward the late Holocene.

#### 4.3.4 Relationships with large-scale climatic changes

The Mediterranean climate results from complex interactions between low- and mid-latitude atmospheric circulations and local features such as orography or land–sea contrast (Brayshaw et al., 2011). The winter Mediterranean hydroclimate depends on the Mediterranean storm activity (and associated precipitation), which is strongly influenced by the position and strength of the mid-latitude North Atlantic (NA) storm track (Brayshaw et al., 2010), while summer dryness is tightly linked to the summer extension and strength of the Hadley cell and associated subtropical subsidence (Lionello et al., 2006). Holocene changes of both NA storm track and tropical convection in response to insolation forcing are therefore critical factors for explaining the long-term climatic evolution in Central Mediterranean and seasonal precipitation changes.

The drier conditions persisting into the early Holocene up to 10.1 ka are also detected in the SW and NE Mediterranean (Kotthoff et al., 2008a; Dormoy et al., 2009). Tzedakis (2007) proposed that early Holocene deficiency in moisture availability is potentially due to the maximum in boreal summer insolation due to strong evaporation. However, seasonal reconstructions show that lower annual precipitation mainly relies on the limitation of winter/fall precipitation (Dormoy et al., 2009; Peyron et al., 2013). Reduced influence of winter westerly flow-induced cyclones on the Mediterranean region appear therefore as a likely cause of the early Holocene delayed afforestation (Kotthoff et al., 2008b). In addition, we have observed that the shift from the GS-1 dry-cold situation to the Holocene warm-humid conditions appears gradual. This may be the result of the progressive reorganisation of the global atmospheric circulation associated with the retreat of Northern Hemisphere ice sheets. The LIS, which disappeared around 6.8 ka (Carlson et al., 2008), was large enough to impact the atmospheric circulation (Montero-Serrano et al., 2010). The Fennoscandian Ice Sheet (FIS), which persisted up to 9 ka, could have influenced the response of the European hydroclimate to insolation forcing in maintaining the NA storm track in a relatively southern position (Magny et al., 2003), although rarely affecting the Mediterranean region before 10.1 ka.

The period comprised between 10.1 and 6.6 ka encompasses the Sapropel 1 (Mercone et al., 2000). Increased precipitation in southern Central Mediterranean is coeval with maximum monsoon activity, as shown by tropical African paleohydrological records (Lézine et al., 2011). However, substantial evidence clearly shows that the African monsoon never reached the Mediterranean region (Tzedakis, 2007). Our data thus confirm these earlier results since the estimated increase in annual precipitation remains limited on average to  $700 \text{ mm an}^{-1}$  in our southern region and mainly due to a change in winter/fall precipitation (Fig. 5). In contrast, monsoonal intensification during summer could have played a predominant role in the Mediterranean summer dry season. Limited summer rainfall in southern Central Mediterranean has been attributed to the development and persistence of subtropical anticyclones as a result of the reinforcement of the Hadley cell related to the African monsoon (Tinner et al., 2009; Gaetani et al., 2011). According to Harrison et al. (1992), the summer northern position and higher strength of the North Atlantic Subtropical High in response to high summer insolation could have blocked the eastward convection into southern Europe. This pattern would explain summer dryness over the whole Central Mediterranean region and the northern progression of summer dryness as observed in pollen and lake level records (Magny et al., 2007a; Finsinger et al., 2010; Peyron et al., 2011).

The winter rainfall maximum from 10.1 to 6.6 ka, observed in the southern Central Mediterranean, appears to be a broad feature of the climate in the Western, Central and North-eastern Mediterranean regions (Fletcher and Sánchez Goñi, 2008; Kotthoff et al., 2008b; Combourieu-Nebout et al., 2009; Dormoy et al., 2009; Jalut et al., 2009; Pérez-Obiol et al., 2011; Peyron et al., 2011). The spatial extent and relative simultaneity of maximum winter rainfalls suggest common mechanisms related to remote controlling factors.

According to Davis and Brewer (2009), the early Holocene increase in moisture availability in the Mediterranean region would be caused by lower evaporation due to cooler conditions, in contrast with our observations. Cool and dry southern conditions would be explained by a more dominant positive Arctic Oscillation/North Atlantic Oscillation (AO/NAO) (Davis and Brewer, 2009) and more northern NA storm track. Bonfils et al. (2004) demonstrated, on the basis of European paleodata, that NAO does not support the winter temperatures and precipitation distribution during the mid-Holocene. They suggest instead an insolation-induced southern entry of the NA storm track in the European mid-latitudes rather than during the late Holocene. Simulations using global and regional models HadSM3 and HadRM3, suggest that increased winter precipitation during the early Holocene would be linked to shifting NA storm track in response to orbital forcing (Brayshaw et al., 2010, 2011). The early–mid Holocene orbital configuration imposes a weaker winter latitudinal insolation gradient that would drive the northern tropical Hadley cell to be narrower and in a more southern position

in winter. Consequently, the NA storm-track would weaken and shift to the south, thus enhancing Mediterranean cyclogenesis and winter precipitation (Brayshaw et al., 2010).

The early Holocene deglaciation of the LIS may have also contributed to increase winter precipitation in the Mediterranean region. The rapid retreat and increased melting of the LIS notably occurred during the wettest phase of the Mediterranean Holocene climate, between 10.0 and 6.8 ka (Carlson et al., 2008). The above mentioned modeling experiment performed by Brayshaw et al. (2010) does not show a significant impact of the LIS on the NA storm track. Another modeling experiment of the “9 ka-climate” with the fully coupled AOGCM ModelE-R, including a more realistic LIS topography and appropriated freshwater routing, showed a stronger impact of the LIS on the North Atlantic oceanic and atmospheric circulation (Carlson et al., 2008). Suppression of the Labrador Sea Water (LSW) formation, substantial reduction of the AMOC (by 15 %), and SST cooling in the NW Atlantic and temperature decrease in NE North America are simulated in agreement with paleodata (Carlson et al., 2008). If effective AMOC reduction is debatable, oceanic circulation reorganisation eventually occurred when LIS retreat had completed (Renssen et al., 2005; Hoogakker et al., 2011). At  $\sim 6.5$  ka, deep water convection in the Nordic Seas reduced and LSW formation reactivated (Hoogakker et al., 2011). According to the ModelE-R experiment, the impact of the LIS melting on atmospheric and North Atlantic circulation induced a southern and stronger NA storm track providing slightly more winter precipitation to mid- and southern Europe (Carlson et al., 2008 (SI: Fig. 4)).

We propose that during the early Holocene, insolation and ice sheets, in particular the LIS decay, modulated winter precipitation in the Western to Central Mediterranean regions by altering oceanic and atmospheric circulation patterns of the North Atlantic, and strengthening the Mediterranean cyclogenesis. After the final demise of the LIS, increase in winter insolation and latitudinal insolation gradient probably contributed to the long-term decrease in winter precipitation and seasonality in the Western and Central Mediterranean by gradually shifting northward the NA storm track, which thus affected less frequently the Mediterranean region.

#### 4.4 Impact of the Holocene centennial-scale climatic changes on temperatures and hydroclimate in the southern Central Mediterranean

The pollen record from core MD047-2497CQ displays a series of eight centennial-scale vegetation changes superimposed on the Holocene long-term evolution. According to our age–depth model, these events occurred at 11.5–11 ka, 10.3–9.9 ka, 9.5–9.1 ka, 8.5–7.9 ka, 7.3–6.7 ka, 6.4–6 ka,  $\sim 5.5$  ka and 4.5 ka.

During the early Holocene dry phase, two centennial-scale dry and cold events at  $\sim 11.2$  ka and 10.1 ka are clearly marked by increases of semi-desert plants with lower tree

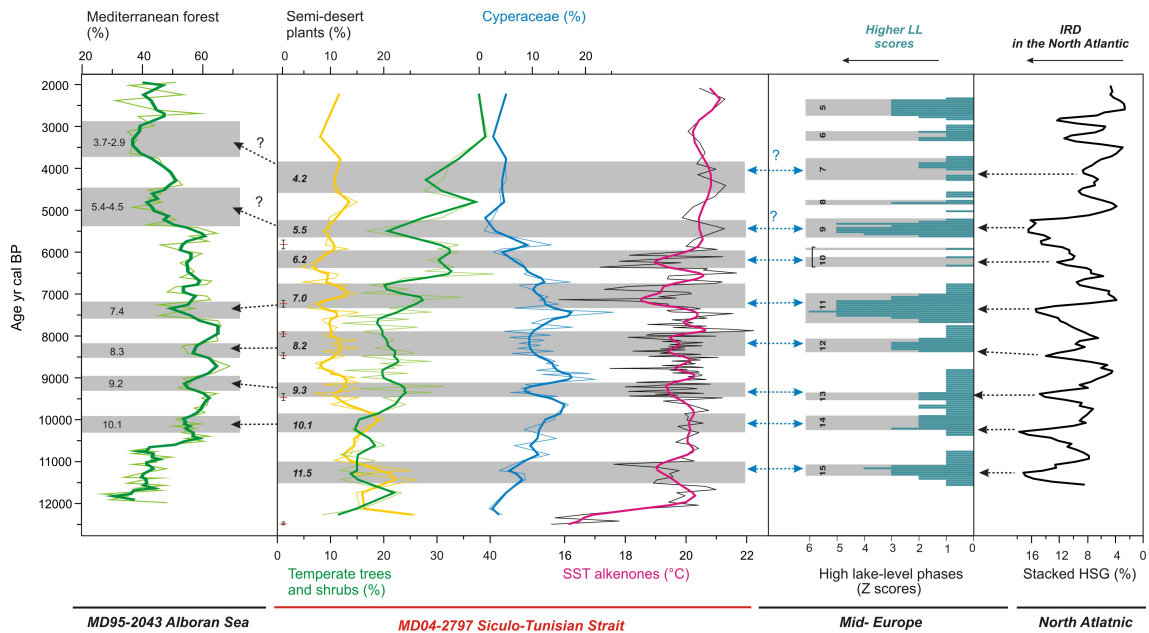


**Fig. 7.** Comparison of the centennial-scale variability recorded in core MD04-2797CQ with changes detected in the Western Mediterranean, middle latitudes of Europe and North Atlantic. From left to right: Mediterranean forest pollen percentages from core MD95-2043 (Fletcher and Sánchez Goñi, 2008): 3-points moving average (bold green line) with forest reduction episodes indicated by the grey bars as in Fletcher et al. (2012); MD04-2797CQ pollen percentages and alkenone-SSTs (bold lines: cubic smoothing splines) with a degree of freedom adjusted to highlight the centennial-scale changes) with abrupt vegetation and SST changes as described in the text; red and black symbols denote radiocarbon age control of core MD04-2797CQ; Mid-European lake level (LL) changes with high lake level phases as indicated in Magny (2013); Stacked Hematite Stained Grains (% HSG) from North Atlantic records (Bond et al., 2001).

and shrubs percentages. During the first event, a large amplitude alkenone-SST cooling is synchronous to vegetation changes, while no SST change is detected during the second one. Further, three SST cooling events at  $\sim 9.3$  ka,  $8.2$  ka,  $7.0$  ka punctuated the wettest Holocene phase ( $10.1$ – $6.6$  ka) and another one occurred at  $\sim 6.2$  ka, the onset of the transition toward drier mid- to late Holocene. All these events are coeval with a change in herbaceous composition, as shown by the strong reductions of Cyperaceae, most of the time replaced by Asteraceae (*Taraxacum*). Strikingly, they do not coincide with trees and shrubs reductions as we would have expected (Fig. 7). For instance, the Mediterranean forest percentages remain stable during the  $9.3$  ka and  $6.2$  ka events while they decline at the end of the  $7.0$  ka event. Different SST and Mediterranean forest variations have also been reported from the Alboran Sea record MD95-2043 (Fletcher et al., 2012), underlying the possible asynchronism between Mediterranean SST millennial-scale cooling and tree development. A seasonal bias towards summer for SST derived from alkenones and winter for the Mediterranean forest is proposed to explain this divergent pattern (Fletcher et al., 2012). However, alkenone-SSTs from core MD04-2797CQ during the interval  $10.1$ – $6.6$  ka do not parallel those found in core MD95-2043, suggesting that they might be controlled by different processes. We will see hereafter that centennial SST coolings from the Siculo-Tunisian Strait are associ-

ated to drier conditions, as revealed by the herbaceous layer changes.

Centennial-scale variations in sedge percentages may have different causes. They could result from variations in the extent of coastal humid areas due to minor sea level changes. Such centennial-scale sea level changes during the early Holocene may be produced by deglacial freshwater pulses, sea-water temperature changes through thermal water expansion or AMOC variations (Levermann et al., 2005; Lombard et al., 2005; Tornqvist and Hijma, 2012). Flooding can also favour sedge development in estuary zones and pollen export to the ocean (Bernhardt et al., 2012). However, high sedge percentages do not coincide with increased periods of flooding, as recorded in the fluvial floodplains of northern Tunisia (Zielhofer and Faust, 2008). On the basis of the whole pollen assemblages, the most straightforward interpretation of sedge reductions is restricted humid areas due to drier conditions. The concomitant *Taraxacum* increase may witness low moisture availability, although relatively weak because semi-desert plants did not expand. In modern pollen assemblages, the highest *Taraxacum* percentages are found in dry environments of Greece and Morocco, where mean annual temperatures span from  $12$  and  $17$  °C and precipitation from  $0$  to  $250$  mm (Leroy, 1997). Therefore, a weak decrease in precipitation and slight cooling, as shown by SSTs remaining above  $16$  °C, would explain why oak populations

were not affected by abrupt climate changes during that period. In contrast, over the last 6 kyr, our pollen record shows two strong abrupt forest reductions around 5.5 ka and 4.5 ka likely resulting from enhanced dryness, even though no SST decreases are recorded.

All the events detected before 6.6 ka parallel, within chronological uncertainties, the widely documented abrupt coolings punctuating the early Holocene: the Preboreal Oscillation (PBO) at  $\sim 11.2$  ka (Björck, 1996); the Boreal Oscillation at  $\sim 10.1$  ka (Björck et al., 2001; Boch et al., 2009); the 9.3 ka event (Rasmussen et al., 2007); the “8.2-event” (Alley et al., 1997); and a final event at  $\sim 7.4$  ka (Bond et al., 2001), which likely corresponds to the drier episode detected at  $\sim 7.0$  ka (Fig. 7). Our pollen record confirms a decrease in precipitation in the Mediterranean region during the early Holocene cooling episodes (Combourieu-Nebout et al., 2009; Dormoy et al., 2009; Pross et al., 2009; Fletcher et al., 2010). In addition, the centennial drier events in our record match the higher lake level episodes in the European mid-latitudes (Magny and Bégeot, 2004) (Fig. 7). This finding supports the early Holocene contrasting pattern of the hydrological changes between the mid-latitudes and southern Europe (Magny and Bégeot, 2004; Fletcher et al., 2012). These cooling events have been associated with deglacial freshwater outbursts in the North Atlantic from proglacial lakes such as Lake Agassiz (Teller et al., 2002), Lake Labrador-Ungava (Jansson and Kleman, 2004), Lake Superior (Yu et al., 2010) or Baltic ice Lake (Nesje et al., 2004), and with solar activity minima (Bond et al., 2001; Magny and Bégeot, 2004). Early Holocene meltwater pulses and solar forcing have been shown to alter the AMOC and modify the atmospheric circulation in the mid-latitudes and also in the tropics (Bond et al., 2001; Magny and Bégeot, 2004; Marchitto et al., 2010). A southern entry point of the Atlantic jet and associated cyclones in Europe and a stronger zonal flow due to enhanced temperature gradient between low and high latitudes are suggested (Magny et al., 2003, 2007b; Magny and Bégeot, 2004).

Abrupt forest reductions at around 5.5 ka and 4.5 ka may be attributed to major widespread cooling events dating to 5.6–5 ka and  $\sim 4.2$  ka, respectively (Magny and Haas, 2004; Drysdale et al., 2006; Magny et al., 2009). This coincidence might be fortuitous because the age control and time resolution of our sequence is low over the last 5.8 kyr. Nevertheless, drier conditions in the southern Mediterranean at  $\sim 5.5$  and 4.2 ka are also suggested by lake-level decreases (Magny et al., 2007a, b). An episode of arboreal biomass reduction at  $\sim 4.2$  ka is recorded in the Central Mediterranean. It has been associated with climate change despite the possible human impact at the beginning of the Bronze Age (Magri and Parra, 2002; Sadori et al., 2011). Both events at  $\sim 5.5$  and 4.2 ka are associated with higher lake levels in the mid-European latitudes and Central Italy in response to North Atlantic cooling and decrease in solar activity (Fig. 7) (Magny, 2004; Magny et al., 2007a). Strikingly, forest reduction episodes in

Western Mediterranean at  $\sim 5.4$ –4.5 ka and 3.7–2.9 ka do not match those events (Fig. 7) (Fletcher et al., 2012). They have been associated to dry conditions in the mid-latitudes and enhanced wind strength in the northern latitudes (Fletcher et al., 2012). However, it is not clear if these forest reduction episodes actually correspond to warm or cold events in the North Atlantic because different timing and periodicity of the centennial-scale variations are recorded in the Alboran Sea pollen sequence and in the North Atlantic IRD record (W. J. Fletcher, personal communication, 2012).

Therefore, given the chronological limitations of our record for this interval, forest reductions in southern Central Mediterranean may be linked either (1) to higher lake level in the mid-European latitude and lower lake level at Lake Preola, or (2) to the forest reduction in the Western Mediterranean. The answer to this question is crucial to the determination of factors controlling the centennial-scale variability during the mid- to late Holocene and their impact on the Mediterranean region. From 6 ka onwards, dry episodes in the southern Central Mediterranean could involve (1) wetter conditions above  $40^\circ$  N due to a southern and stronger Atlantic jet like during the early Holocene cooling events (Magny and Bégeot, 2004) or (2) drier conditions in the Mediterranean and mid-European latitudes due to an intensification and northward shift of the NA storm track and subsequent limited penetration of storms in the Mediterranean region (Fletcher et al., 2012).

Apart from this, our record as well as the MD95-2043 pollen sequence (Fig. 7) shows that changes on land are of weaker amplitude during the early Holocene, in particular during Sapropel 1, as compared to the mid- to late Holocene. The notable weak expression of the 8.2 event in the Central Mediterranean has already been emphasized from the Accesa and Preola sequences (Fig. 1) (Magny et al., 2011b; Peyron et al., 2011). This event is even missing in Moroccan and Tunisian alluvial sequences (Zielhofer et al., 2008). This finding emphasizes that impact of cooling events in the early Holocene was relatively weak on the Western to Central Mediterranean hydroclimate, while changes were apparently stronger during the mid- to late Holocene.

Despite increased dryness, paleodata suggest that NA storms were still substantially affecting southern Europe during the early Holocene cooling events, though to a lesser extent than during the bracketing warm phases. In a context where NA storm track is in a mean southern position caused by insolation and LIS melt forcing, cooling events in the North Atlantic may have produced stronger and more zonal cyclones, enhancing precipitation at mid-latitudes and somewhat restricting them in southern Europe. In contrast, during the mid- to late Holocene, in the absence of ice sheet forcing, the NA storm tracks were likely more northern, thus less frequently affecting southern Europe. Therefore, centennial-scale variations may have induced stronger aridity in the Mediterranean region. Baseline climate states, such as insolation and ice sheet extent, exert a strong control on

the atmospheric circulation in the North Atlantic and thus likely modulate the impact of abrupt climate changes on the Mediterranean region.

## 5 Conclusions

The deglacial and Holocene climate of the southern Central Mediterranean are examined at orbital and millennial to centennial time-scale using a marine pollen record (MD04-2797CQ). Our reconstruction provides an integrated picture of the regional vegetation changes and main regional climate features over the last 18 200 yr:

- Prevailing dry conditions during the deglaciation are indicated by the dominance of semi-desert plants. Conditions remained arid even during the GI-1, restricting the expansion of the trees and shrubs despite climatic amelioration.
- Our land–sea correlation shows with no chronological ambiguity that even though temperatures increased at the GS-1 – Holocene transition in the southern Central Mediterranean, tree and shrub expansion was strongly limited by moisture deficiency persisting into the early Holocene up to 10.1 ka.
- Temperate trees and shrubs with heaths in the oak forest understory and heath maquis expanded between 10.1 and 6.6 ka while Mediterranean plants only developed from 6.6 ka to the late Holocene. Climate in southern Central Mediterranean was wetter during the early Holocene interval, corresponding to Sapropel 1, and became drier during the mid- to late Holocene, mainly because of a change in winter precipitation while summers remained dry.

Our findings suggest, in agreement with previous modeling experiments, that the Holocene long-term winter precipitation changes in the Mediterranean region depends on the mid-latitude atmospheric circulation, which is basically controlled by insolation and ice sheet dynamics. In particular, increased melting rate of the LIS between 10 and 6.8 ka combined with weak winter insolation played a major role in the Mediterranean winter precipitation maxima during the early Holocene. This feature is likely related to more frequent NA storm tracks in a mean southern position, feeding the Mediterranean cyclogenesis, than during the mid- to late Holocene.

Finally, our data provide evidence for the impact of Holocene centennial-scale climate changes on the Central Mediterranean vegetation (11.5–11 ka, 10.3–9.9 ka, 9.5–9.1 ka, 8.5–7.9 ka, 7.3–6.7 ka, 6.4–6 ka, and at around 5.5 ka and 4.5 ka). The lack of response of the Mediterranean forest but detection of herbaceous composition changes during the wet early Holocene indicate muted changes in precipitation contrasting with episodes of enhanced aridity dur-

ing the mid- to late Holocene. We suggest that the impact of the Holocene centennial-scale variability results from baseline climate states, insolation and ice sheet extent, shaping the response of the mid-latitudes atmospheric circulation.

*Acknowledgements.* Financial support was provided by the ANR LAMA. We thank logistics and coring teams on board the R/V *Marion Dufresne II* during the PRIVILEGE-PRIMAROSA oceanographic cruise. We are grateful to Murielle Georget and Marie-Hélène Castera for technical assistance. We gratefully acknowledge Maria Fernanda Sanchez Goñi, Anne-Laure Daniau and William J. Fletcher for support and discussions as well as Michel Magny for comments on the manuscript and coordination of the LAMA project. We thank W. Tinner, L. Sadori, D. Genty, W. J. Fletcher and M. Magny for sharing paleodata. This is LSCE contribution no. 4583

Edited by: M. Magny



The publication of this article is financed by CNRS-INSU.

## References

- Allen, J. R. M., Watts, W. A., McGee, E., and Huntley, B.: Holocene environmental variability – The record from Lago Grande di Monticchio, Italy, *Quaternary Int.*, 88, 69–80, 2002.
- Alley, R. B., Mayewski, P. A., Sowers, T., Stuiver, M., Taylor, K. C., and Clark, P. U.: Holocene climatic instability: A prominent, widespread event 8200 yr ago, *Geology*, 25, 483–486, 1997.
- Astraldi, M., Gasparini, G. P., Vetrano, A., and Vignudelli, S.: Hydrographic characteristics and interannual variability of water masses in the central Mediterranean: a sensitivity test for long-term changes in the Mediterranean Sea, *Deep Sea Res. Part I*, 49, 661–680, doi:10.1016/s0967-0637(01)00059-0, 2002.
- Bard, E., Rostek, F., Turon, J. L., and Gendreau, S.: Hydrological impact of Heinrich events in the subtropical northeast Atlantic, *Science*, 289, 1321–1324, 2000.
- Ben Tiba, B.: Cinq millénaires d’histoire de la végétation à Djebel El Ghorra, Tunisie septentrionale, *Symposium de Palynologie africaine*, Tervuren, Belgique, 49–55, 1995.
- Ben Tiba, B. and Reille, M.: Recherches pollenanalytiques dans les montagnes de Kroumirie (Tunisie septentrionale): Premiers résultats, *Ecologia Mediterranea*, 8, 75–86, 1982.
- Béranger, K., Mortier, L., Gasparini, G. P., Gervasio, L., Astraldi, M., and Crépon, M.: The dynamics of the Sicily Strait: A comprehensive study from observations and models, *Deep-Sea Res. Part II*, 51, 411–440, 2004.
- Berger, A. and Loutre, M. F.: Insolation values for the climate of the last 10 million years, *Quaternary Sci. Rev.*, 10, 297–317, 1991.

- Bernhardt, C. E., Horton, B. P., and Stanley, J. D.: Nile Delta vegetation response to Holocene climate variability, *Geology*, 40, 615–618, 2012.
- Björck, S.: Synchronized terrestrial-atmospheric deglacial records around the North Atlantic, *Science*, 274, 1155–1160, 1996.
- Björck, S., Muscheler, R., Kromer, B., Andresen, C. S., Heinemeier, J., Johnsen, S. J., Conley, D., Koç, N., Spurk, M., and Veski, S.: High-resolution analyses of an early Holocene climate event may imply decreased solar forcing as an important climate trigger, *Geology*, 29, 1107–1110, doi:10.1130/0091-7613(2001)029<1107:hraoae>2.0.co;2, 2001.
- Boch, R., Spötl, C., and Kramers, J.: High-resolution isotope records of early Holocene rapid climate change from two coeval stalagmites of Katerloch Cave, Austria, *Quaternary Sci. Rev.*, 28, 2527–2538, doi:10.1016/j.quascirev.2009.05.015, 2009.
- Bond, G. and Lotti, R.: Icebergs discharges into the North Atlantic on millennial time scales during the Last Glaciation, *Science*, 267, 1005–1009, 1995.
- Bond, G., Showers, W., Cheseby, M., Lotti, R., Almasi, P., deMenocal, P., Priore, P., Cullen, H., Hajdas, I., and Bonani, G.: A pervasive millennial-scale cycle in North Atlantic Holocene and Glacial Climates, *Science*, 278, 1257–1266, 1997.
- Bond, G., Kromer, B., Beer, J., Muscheler, R., Evans, M. N., Showers, W., Hoffman, S., Lotti-Bond, R., Hajdas, I., and Bonani, G.: Persistent solar influence on North Atlantic climate during the Holocene, *Science*, 294, 2130–2136, 2001.
- Bonfils, C., de Noblet-Ducoudré, N., Guiot, J., and Bartlein, P.: Some mechanisms of mid-Holocene climate change in Europe, inferred from comparing PMIP models to data, *Clim. Dynam.*, 23, 79–98, 2004.
- Boussaid, M., Ben Fadhel, N., Chemli, R., and Ben M'hamed, M.: Structure of vegetation in Northern and Central Tunisia and protective measures, in: *Wild food and non-food plants: Information networking*, edited by: Heywood, V. H. and Skoula, M., Cahiers Options Méditerranéennes, CIHEAM, 295–302, 1999.
- Bout-Roumazeilles, V., Combourieu-Nebout, N., Desprat, S., Es-sallami, L., Siani, G., and Turon, J. L.: Tracking atmospheric and riverine terrigenous supplies variability during the Holocene and last glacial in central Mediterranean, *Clim. Past*, in review, 2013.
- Braconnot, P., Otto-Bliesner, B., Harrison, S., Joussaume, S., Peterchmitt, J.-Y., Abe-Ouchi, A., Crucifix, M., Driesschaert, E., Fichefet, Th., Hewitt, C. D., Kageyama, M., Kitoh, A., Laîné, A., Loutre, M.-F., Marti, O., Merkel, U., Ramstein, G., Valdes, P., Weber, S. L., Yu, Y., and Zhao, Y.: Results of PMIP2 coupled simulations of the Mid-Holocene and Last Glacial Maximum – Part 1: experiments and large-scale features, *Clim. Past*, 3, 261–277, doi:10.5194/cp-3-261-2007, 2007.
- Brayshaw, D. J., Hoskins, B., and Black, E.: Some physical drivers of changes in the winter storm tracks over the North Atlantic and Mediterranean during the Holocene, *Philos. T. R. Soc. A*, 368, 5185–5223, 2010.
- Brayshaw, D. J., Rambeau, C. M. C., and Smith, S. J.: Changes in mediterranean climate during the holocene: Insights from global and regional climate modelling, *The Holocene*, 21, 15–31, 2011.
- Broecker, W. S.: Was the Younger Dryas triggered by a flood?, *Science*, 312, 1146–1148, 2006.
- Brun, A.: Recherches palynologiques sur les sédiments du Golfe de Gabès: résultats préliminaires, *Géologie méditerranéenne: la Mer Pélagienne*, Marseille, 1979,
- Brun, A.: Etude palynologique des sédiments marins Holocènes de 5000 B.P. à l'actuel dans le Golfe de Gabès (Mer Pélagienne), *Pollen et Spores*, 25, 437–460, 1983.
- Brun, A.: La couverture steppique en Tunisie au Quaternaire supérieur, *Comptes Rendus – Academie des Sciences, Serie II*, 14, 1085–1090, 1985.
- Cacho, I., Grimalt, J. O., Canals, M., Sbaiffi, L., Shackleton, N. J., Schönfeld, J., and Zahn, R.: Variability of the Western Mediterranean sea surface temperature during the last 25,000 years and its connection with the Northern Hemisphere climatic changes, *Paleoceanography*, 16, 40–52, 2001.
- Calò, C., Henne, P. D., Curry, B., Magny, M., Vescovi, E., La Mantia, T., Pasta, S., Vannièrè, B., and Tinner, W.: Spatio-temporal patterns of Holocene environmental change in southern Sicily, *Palaeogeogr. Palaeoecol.*, 323–325, 110–122, doi:10.1016/j.palaeo.2012.01.038, 2012.
- Carlson, A. E., Legrande, A. N., Oppo, D. W., Came, R. E., Schmidt, G. A., Anslow, F. S., Licciardi, J. M., and Obbink, E. A.: Rapid early Holocene deglaciation of the Laurentide ice sheet, *Nat. Geosci.*, 1, 620–624, 2008.
- Chronis, T., Papadopoulos, V., and Nikolopoulos, E. I.: QuickSCAT observations of extreme wind events over the Mediterranean and Black Seas during 2000–2008, *Int. J. Climatol.*, 31, 2068–2077, doi:10.1002/joc.2213, 2011.
- Combourieu-Nebout, N., Paterne, M., Turon, J.-L., and Siani, G.: A high-resolution record of the Last Deglaciation in the central Mediterranean sea: Palaeovegetation and palaeohydrological evolution, *Quaternary Sci. Rev.*, 17, 303–332, 1998.
- Combourieu Nebout, N., Peyron, O., Dormoy, I., Desprat, S., Beaudouin, C., Kotthoff, U., and Marret, F.: Rapid climatic variability in the west Mediterranean during the last 25 000 years from high resolution pollen data, *Clim. Past*, 5, 503–521, doi:10.5194/cp-5-503-2009, 2009.
- Combourieu-Nebout, N.: Central Mediterranean vegetation and climate changes during the Holocene through pollen records around the Adriatic Sea, *Clim. Past Discuss.*, in preparation, 2013.
- Correa-Metrio, A., Urrego, D. H., Cabrera, B., and Bush, M.: paleoMAS: Paleocological Analysis. R package version 2.0, The Comprehensive R Archive Network, 2011.
- Davis, B. A. S. and Brewer, S.: Orbital forcing and role of the latitudinal insolation/temperature gradient, *Clim. Dynam.*, 32, 143–165, 2009.
- De Beaulieu, J. L., Miras, Y., Andrieu-Ponel, V., and Guiter, F.: Vegetation dynamics in north-western Mediterranean regions: Instability of the Mediterranean bioclimate, *Plant Biosyst.*, 139, 114–126, 2005.
- Di Rita, F. and Magri, D.: Holocene drought, deforestation and evergreen vegetation development in the central Mediterranean: A 5500 year record from Lago Alimini Piccolo, Apulia, southeast Italy, *Holocene*, 19, 295–306, 2009.
- Dormoy, I., Peyron, O., Combourieu Nebout, N., Goring, S., Kotthoff, U., Magny, M., and Pross, J.: Terrestrial climate variability and seasonality changes in the Mediterranean region between 15 000 and 4000 years BP deduced from marine pollen records, *Clim. Past*, 5, 615–632, doi:10.5194/cp-5-615-2009, 2009.
- Drysdale, R., Zanchetta, G., Hellstrom, J., Maas, R., Fallick, A., Pickett, M., Cartwright, I., and Piccini, L.: Late Holocene drought responsible for the collapse of Old World civilizations is recorded in an Italian cave flowstone, *Geology*, 34, 101–104,

- 2006.
- Dupont, L. and Wyputta, U.: Reconstructing pathways of aeolian pollen transport to the marine sediments along the coastline of SW Africa, *Quaternary Sci. Rev.*, 22, 157–174, 2003.
- El Euch, F.: Le sylvopastoralisme en Tunisie, in: *Sylvopastoral systems. Environmental, agricultural and economic sustainability*, Cahiers Options Méditerranéennes, CIHEAM, Zaragoza, 1995.
- Essallami, L., Sicre, M. A., Kallel, N., Labeyrie, L., and Siani, G.: Hydrological changes in the Mediterranean Sea over the last 30,000 years, *Geochem. Geophys. Geosyst.*, 8, Q07002, doi:10.1029/2007gc001587, 2007.
- Finné, M., Holmgren, K., Sundqvist, H. S., Weiberg, E., and Lindblom, M.: Climate in the eastern Mediterranean, and adjacent regions, during the past 6000 years – A review, *Journal of Archaeological Science*, 38, 3153–3173, doi:10.1016/j.jas.2011.05.007, 2011.
- Finsinger, W., Colombaroli, D., De Beaulieu, J. L., Valsecchi, V., Vannièrre, B., Vescovi, E., Chapron, E., Lotter, A. F., Magny, M., and Tinner, W.: Early to mid-Holocene climate change at Lago dell'Accesa (central Italy): Climate signal or anthropogenic bias?, *J. Quaternary Sci.*, 25, 1239–1247, 2010.
- Finsinger, W., Lane, C. S., van Den Brand, G. J., Wagner-Cremer, F., Blockley, S. P. E., and Lotter, A. F.: Theateglacial Quercus expansion in the southern European Alps: Rapid vegetation response to a late Allerød climate warming?, *J. Quaternary Sci.*, 26, 694–702, 2011.
- Fletcher, W. J. and Sánchez Goñi, M. F.: Orbital- and sub-orbital-scale climate impacts on vegetation of the western Mediterranean basin over the last 48,000 yr, *Quaternary Res.*, 70, 451–464, 2008.
- Fletcher, W. J. and Zielhofer, C.: Fragility of Western Mediterranean landscapes during Holocene Rapid Climate Changes, *Catena*, 103, 16–29, 2011.
- Fletcher, W. J., Sanchez Goñi, M. F., Peyron, O., and Dormoy, I.: Abrupt climate changes of the last deglaciation detected in a Western Mediterranean forest record, *Clim. Past*, 6, 245–264, doi:10.5194/cp-6-245-2010, 2010.
- Fletcher, W. J., Debret, M., and Sanchez Goñi, M. F.: Mid-Holocene emergence of a low-frequency millennial oscillation in western Mediterranean climate: implications for past dynamics of the North Atlantic atmospheric westerlies, *The Holocene*, 23, 153–166, doi:10.1177/0959683612460783, 2012.
- Frisia, S., Borsato, A., Mangini, A., Spötl, C., Madonia, G., and Sauro, U.: Holocene climate variability in Sicily from a discontinuous stalagmite record and the Mesolithic to Neolithic transition, *Quaternary Res.*, 66, 388–400, 2006.
- Gaetani, M., Pohl, B., Douville, H., and Fontaine, B.: West African Monsoon influence on the summer Euro-Atlantic circulation, *Geophys. Res. Lett.*, 38, L09705, doi:10.1029/2011GL047150, 2011.
- Gausson, H. and Vernet, A.: *Carte Internationale du Tapis Végétal. Tunis-Sfax*, Institut Géographique National, Paris, Gouvernement Tunisien, 1958.
- Genty, D., Blamart, D., Ghaleb, B., Plagnes, V., Causse, C., Bakalowicz, M., Zouari, K., Chkir, N., Hellstrom, J., Wainer, K., and Bourges, F.: Timing and dynamics of the last deglaciation from European and North African  $\delta^{13}\text{C}$  stalagmite profiles – comparison with Chinese and South Hemisphere stalagmites, *Quaternary Sci. Rev.*, 25, 2118–2142, doi:10.1016/j.quascirev.2006.01.030, 2006.
- Giorgi, F.: Climate change hot-spots, *Geophys. Res. Lett.*, 33, L08707, doi:10.1029/2006GL025734, 2006.
- Guiot, J.: Methodology of the last climatic cycle reconstruction from pollen data, *Palaeogeogr. Palaeoclimatol.*, 80, 49–69, 1990.
- Harrison, S. P., Prentice, I. C., and Bartlein, P. J.: Influence of insolation and glaciation on atmospheric circulation in the North Atlantic sector: Implications of general circulation model experiments for the Late Quaternary climatology of Europe, *Quaternary Sci. Rev.*, 11, 283–299, 1992.
- Heusser, L. E.: Spores and pollen in the marine realm, in: *Introduction to marine micropaleontology*, edited by: Haq, B. U. and Boersma, A., Elsevier, New York, 327–339, 1978.
- Heusser, L. E. and Balsam, W. L.: Pollen distribution in the N.E. Pacific ocean, *Quaternary Res.*, 7, 45–62, 1977.
- Hoogakker, B. A. A., Chapman, M. R., McCave, I. N., Hillaire-Marcel, C., Ellison, C. R. W., Hall, I. R., and Telford, R. J.: Dynamics of North Atlantic Deep Water masses during the Holocene, *Paleoceanography*, 26, PA4214, doi:10.1029/2011PA002155, 2011.
- INRF: *Carte Bioclimatique de la Tunisie selon la classification d'Emberger, Etages et Variantes*, Institut National de Recherches Forestières, République Tunisienne, 1976.
- IPCC: *Climate Change 2007: Synthesis Report. Contribution of Working Groups I, II and III to the Fourth Assessment Report of the Intergovernmental Panel on Climate Change*, Geneva, Switzerland, 104 pp., 2007.
- Jalut, G., Esteban Amat, A., Bonnet, L., Gauquelin, T., and Fontugne, M.: Holocene climatic changes in the Western Mediterranean, from south-east France to south-east Spain, *Palaeogeogr. Palaeoclimatol.*, 160, 255–290, 2000.
- Jalut, G., Dedoubat, J. J., Fontugne, M., and Otto, T.: Holocene circum-Mediterranean vegetation changes: Climate forcing and human impact, *Quaternary Int.*, 200, 4–18, doi:10.1016/j.quaint.2008.03.012, 2009.
- Jansson, K. N. and Kleman, J.: Early Holocene glacial lake meltwater injections into the Labrador Sea and Ungava Bay, *Paleoceanography*, 19, PA1001, doi:10.1029/2003PA000943, 2004.
- Johnsen, S. J., Clausen, H. B., Dansgaard, W., Fuhrer, K., Gundestrup, N., Hammer, C. U., Iversen, P., Jouzel, J., Stauffer, B., and Steffensen, J. P.: Irregular glacial interstadials recorded in a new Greenland ice core, *Nature*, 359, 311–313, 1992.
- Juggins, S.: *Package "rioja" – Analysis of Quaternary Science Data*, The Comprehensive R Archive Network, 2009.
- Kotthoff, U., Müller, U. C., Pross, J., Schmiiedl, G., Lawson, I. T., Van De Schootbrugge, B., and Schulz, H.: Lateglacial and Holocene vegetation dynamics in the Aegean region: An integrated view based on pollen data from marine and terrestrial archives, *Holocene*, 18, 1019–1032, 2008a.
- Kotthoff, U., Pross, J., Müller, U. C., Peyron, O., Schmiiedl, G., Schulz, H., and Bordon, A.: Climate dynamics in the borderlands of the Aegean Sea during formation of sapropel S1 deduced from a marine pollen record, *Quaternary Sci. Rev.*, 27, 832–845, doi:10.1016/j.quascirev.2007.12.001, 2008b.
- Lambeck, K., Antonioli, F., Purcell, A., and Silenzi, S.: Sea-level change along the Italian coast for the past 10,000 yr, *Quaternary Sci. Rev.*, 23, 1567–1598, doi:10.1016/j.quascirev.2004.02.009, 2004.

- Leroy, S. A. G.: Climatic and non-climatic lake-level changes inferred from a Plio-Pleistocene lacustrine complex of Catalonia (Spain): palynology of the Tres Pins sequences, *J. Paleolimnol.*, 17, 347–367, 1997.
- Levermann, A., Griesel, A., Hofmann, M., Montoya, M., and Rahmstorf, S.: Dynamic sea level changes following changes in the thermohaline circulation, *Clim. Dynam.*, 24, 347–354, doi:10.1007/s00382-004-0505-y, 2005.
- Lézine, A. M., Hély, C., Grenier, C., Braconnot, P., and Krinner, G.: Sahara and Sahel vulnerability to climate changes, lessons from Holocene hydrological data, *Quaternary Sci. Rev.*, 30, 3001–3012, 2011.
- Lionello, P., Malanotte-Rizzoli, P., Boscolo, R., Alpert, P., Artale, V., Li, L., Luterbacher, J., May, W., Trigo, R., Tsimplis, M., Ulbrich, U., and Xoplaki, E.: The Mediterranean climate: An overview of the main characteristics and issues, in: *Developments in Earth and Environmental Sciences*, edited by: P. Lionello, P. M.-R. and Boscolo, R., Elsevier, 1–26, 2006.
- Lombard, A., Cazenave, A., DoMinh, K., Cabanes, C., and Nerem, R. S.: Thermosteric sea level rise for the past 50 years; comparison with tide gauges and inference on water mass contribution, *Global Planet. Change*, 48, 303–312, doi:10.1016/j.gloplacha.2005.02.007, 2005.
- Lowe, J. J., Rasmussen, S. O., Björck, S., Hoek, W. Z., Steffensen, J. P., Walker, M. J. C., and Yu, Z. C.: Synchronisation of palaeoenvironmental events in the North Atlantic region during the Last Termination: a revised protocol recommended by the INTIMATE group, *Quaternary Sci. Rev.*, 27, 6–17, doi:10.1016/j.quascirev.2007.09.016, 2008.
- Lundqvist, J. and Saarnisto, M.: Summary of project IGCP-253, *Quaternary Int.*, 28, 9–18, 1995.
- MacAyeal, D. R.: Binge/purge oscillations of the Laurentide ice sheet as a cause of the north Atlantic's heinrich events, *Paleoceanography*, 8, 775–785, 1993.
- Magny, M.: Holocene climate variability as reflected by mid-European lake-level fluctuations and its probable impact on pre-historic human settlements, *Quaternary Int.*, 113, 65–79, 2004.
- Magny, M.: Orbital, ice-sheet, and possible solar forcing of Holocene lake-level fluctuations in west-central Europe. A comment on Bleicher (2013) *The Holocene*, in press, 2013.
- Magny, M. and Bégeot, C.: Hydrological changes in the European midlatitudes associated with freshwater outbursts from Lake Agassiz during the Younger Dryas event and the early Holocene, *Quaternary Res.*, 61, 181–192, 2004.
- Magny, M. and Haas, J. N.: A major widespread climatic change around 5300 cal. yr BP at the time of the Alpine Iceman, *J. Quaternary Sci.*, 19, 423–430, 2004.
- Magny, M., Bégeot, C., Guiot, J., and Peyron, O.: Contrasting patterns of hydrological changes in Europe in response to Holocene climate cooling phases, *Quaternary Sci. Rev.*, 22, 1589–1596, 2003.
- Magny, M., de Beaulieu, J. L., Drescher-Schneider, R., Vannièrè, B., Walter-Simonnet, A. V., Miras, Y., Millet, L., Bossuet, G., Peyron, O., Brugiapaglia, E., and Leroux, A.: Holocene climate changes in the central Mediterranean as recorded by lake-level fluctuations at Lake Accessa (Tuscany, Italy), *Quaternary Sci. Rev.*, 26, 1736–1758, 2007a.
- Magny, M., Vannièrè, B., de Beaulieu, J. L., Bégeot, C., Heiri, O., Millet, L., Peyron, O., and Walter-Simonnet, A. V.: Early-Holocene climatic oscillations recorded by lake-level fluctuations in west-central Europe and in central Italy, *Quaternary Sci. Rev.*, 26, 1951–1964, 2007b.
- Magny, M., Vannièrè, B., Zanchetta, G., Fouache, E., Touchais, G., Petrika, L., Coussot, C., Walter-Simonnet, A. V., and Arnaud, F.: Possible complexity of the climatic event around 4300–3800 cal. BP in the central and western Mediterranean, *Holocene*, 19, 823–833, 2009.
- Magny, M., Peyron, O., Sadori, L., Ortu, E., Zanchetta, G., Vannièrè, B., and Tinner, W.: Contrasting patterns of precipitation seasonality during the Holocene in the south- and north-central Mediterranean, *J. Quaternary Sci.*, 27, 290–296, 2011a.
- Magny, M., Vannièrè, B., Calò, C., Millet, L., Leroux, A., Peyron, O., Zanchetta, G., La Mantia, T., and Tinner, W.: Holocene hydrological changes in south-western Mediterranean as recorded by lake-level fluctuations at Lago Preola, a coastal lake in southern Sicily, Italy, *Quaternary Sci. Rev.*, 30, 2459–2475, doi:10.1016/j.quascirev.2011.05.018, 2011b.
- Magri, D.: Late Quaternary vegetation history at Lagaccione near Lago di Bolsena (central Italy), *Rev. Palaeobot. Palynol.*, 106, 171–208, 1999.
- Magri, D. and Sadori, L.: Late Pleistocene and Holocene pollen stratigraphy at Lago di Vico, central Italy, *Veg. His. Archaeobot.*, 8, 247–260, 1999.
- Magri, D. and Parra, I.: Late Quaternary western Mediterranean pollen records and African winds, *Earth Planet. Sci. Lett.*, 200, 401–408, 2002.
- Marchitto, T. M., Muscheler, R., Ortiz, J. D., Carriquiry, J. D., and Van Geen, A.: Dynamical response of the tropical Pacific ocean to solar forcing during the early Holocene, *Science*, 330, 1378–1381, 2010.
- McManus, J. F., Francois, R., Gherardi, J.-M., Keigwin, L. D., and Brown-Leger, S.: Collapse and rapid resumption of Atlantic meridional circulation linked to deglacial climate changes, *Nature*, 428, 834–837, 2004.
- Médail, F. and Diadema, K.: Glacial refugia influence plant diversity patterns in the Mediterranean Basin, *J. Biogeogr.*, 36, 1333–1345, 2009.
- Mercone, D., Thomson, J., Croudace, I. W., Siani, G., Paterne, M., and Troelstra, S.: Duration of S1, the most recent sapropel in the eastern Mediterranean Sea, as indicated by accelerator mass spectrometry radiocarbon and geochemical evidence, *Paleoceanography*, 15, 336–347, 2000.
- Montero-Serrano, J. C., Bout-Roumazielles, V., Sionneau, T., Tribouillard, N., Bory, A., Flower, B. P., Riboulleau, A., Martinez, P., and Billy, I.: Changes in precipitation regimes over North America during the Holocene as recorded by mineralogy and geochemistry of Gulf of Mexico sediments, *Global Planet. Change*, 74, 132–143, 2010.
- Naughton, F., Sanchez Goni, M. F., Desprat, S., Turon, J.-L., Duprat, J., Malaize, B., Joli, C., Cortijo, E., Drago, T., and Freitas, M. C.: Present-day and past (last 25 000 years) marine pollen signal off western Iberia, *Mar. Micropaleontol.*, 62, 91–114, 2007.
- Nesje, A., Dahl, S. O., and Bakke, J.: Were abrupt Lateglacial and early-Holocene climatic changes in northwest Europe linked to freshwater outbursts to the North Atlantic and Arctic Oceans?, *Holocene*, 14, 299–310, 2004.

- NGRIP members: High-resolution record of northern hemisphere climate extending into the last interglacial period, *Nature*, 431, 147–151, 2004.
- Noti, R., van Leeuwen, J. F. N., Colombaroli, D., Vescovi, E., Pasta, S., la Mantia, T., and Tinner, W.: Mid- and late-holocene vegetation and fire history at Biviere di Gela, a coastal lake in southern Sicily, Italy, *Veg. Hist. Archaeobot.*, 18, 371–387, 2009.
- Ojeda, F., Arroyo, J., and Marañón, T.: The phytogeography of European and Mediterranean heath species (Ericoideae, Ericaceae): A quantitative analysis, *J. Biogeogr.*, 25, 165–178, 1998.
- Pérez-Obiol, R., Jalut, G., Julià, R., Pèlachs, A., Iriarte, M. J., Otto, T., and Hernández-Beloqui, B.: Mid-holocene vegetation and climatic history of the Iberian peninsula, *The Holocene*, 21, 75–93, 2011.
- Peterson, L. C., Haug, G. H., Hughen, K. A., and Rohl, U.: Rapid changes in the hydrologic cycle of the tropical Atlantic during the last glacial, *Science*, 290, 1947–1951, 2000.
- Peyron, O., Goring, S., Dormoy, I., Kotthoff, U., Pross, J., de Beaulieu, J. L., Drescher-Schneider, R., Vannié, B., and Magny, M.: Holocene seasonality changes in the central Mediterranean region reconstructed from the pollen sequences of Lake Accesa (Italy) and Tenaghi Philippon (Greece), *The Holocene*, 21, 131–146, 2011.
- Peyron, O., Magny, M., Goring, S., Joannin, S., de Beaulieu, J.-L., Brugiapaglia, E., Sadori, L., Garfi, G., Kouli, K., Ioakim, C., and Combourieu-Nebout, N.: Contrasting patterns of climatic changes during the Holocene in the Central Mediterranean (Italy) reconstructed from pollen data, *Clim. Past Discuss.*, 8, 5817–5866, doi:10.5194/cpd-8-5817-2012, 2012.
- Peyron, O., Combourieu-Nebout, N., Magny, M., Goring, S., Joannin, S., Dormoy, I., Brayshaw, D., de Beaulieu, J.-L., Brugiapaglia, E., Desprat, S., Kouli, K., Kotthoff, U., Pross, J., and Sadori, L.: Holocene climate changes in Mediterranean area: a model-data comparison, *Clim. Past*, in preparation, 2013.
- Pinardi, N., Zavatarelli, M., Arneri, E., Crise, A., and Ravaioli, M.: The Physical sedimentary and ecological structure and variability of shelf areas in the Mediterranean Sea, in: *The global coastal ocean – Interdisciplinary regional studies and syntheses*, edited by: Robinson, A. R. and Brink, K. H., Harvard University Press, Cambridge, MA and London, 1245–1331, 2005.
- Posner, S. D.: *Biological diversity and tropical forests in Tunisia*, Agency for International Development, 206 pp., 1988.
- Pross, J., Kotthoff, U., Müller, U. C., Peyron, O., Dormoy, I., Schmiel, G., Kalaitzidis, S., and Smith, A. M.: Massive perturbation in terrestrial ecosystems of the Eastern Mediterranean region associated with the 8.2 kyr B.P. climatic event, *Geology*, 37, 887–890, 2009.
- Quezel, P.: *Réflexions sur l'évolution de la flore et de la végétation au Maghreb méditerranéen*, Ibis Press, 2002.
- Ramdani, M., Flower, R. J., Elkhiati, N., Kraïem, M. M., Fathi, A. A., Birks, H. H., and Patrick, S. T.: North African wetland lakes: characterization of nine sites included in the CASSARINA Project, *Aquat. Ecol.*, 35, 281–302, 2001.
- Rasmussen, S. O., Andersen, K. K., Svensson, A. M., Steffensen, J. P., Vinther, B. M., Clausen, H. B., Siggaard-Andersen, M.-L., Johnsen, S. J., Larsen, L. B., Dahl-Jensen, D., Bigler, M., Röthlisberger, R., Fischer, H., Goto-Azuma, K., Hansson, M. E., and Ruth, U.: A new Greenland ice core chronology for the last glacial termination, *J. Geophys. Res.*, 111, D06102, doi:10.1029/2005JD006079, 2006.
- Rasmussen, S. O., Vinther, B. M., Clausen, H. B., and Andersen, K. K.: Early Holocene climate oscillations recorded in three Greenland ice cores, *Quaternary Sci. Rev.*, 26, 1907–1914, 2007.
- Rasmussen, S. O., Seierstad, I. K., Andersen, K. K., Bigler, M., Dahl-Jensen, D., and Johnsen, S. J.: Synchronization of the NGRIP, GRIP, and GISP2 ice cores across MIS 2 and palaeoclimatic implications, *Quaternary Sci. Rev.*, 27, 18–28, 2008.
- Reimer, P. J., Baillie, M. G. L., Bard, E., Bayliss, A., Beck, J. W., Blackwell, P. G., Bronk Ramsey, C., Buck, C. E., Burr, G., Edwards, R. L., Friedrich, M., Grootes, P. M., Guilderson, T. P., Hajdas, I., Heaton, T. J., Hogg, A. G., Hughen, K. A., Kaiser, K. F., Kromer, B., McCormac, F. G., Manning, S. W., Reimer, R. W., Richards, D. A., Southon, J., Turney, C. S. M., van der Plicht, J., and Weyhenmeyer, C.: IntCal09 and Marine09 radiocarbon age calibration curves, 0–50,000 years cal BP, *Radiocarbon*, 51, 1111–1150, 2009.
- Renssen, H., Goosse, H., and Fichet, T.: Contrasting trends in North Atlantic deep-water formation in the Labrador Sea and Nordic Seas during the Holocene, *Geophys. Res. Lett.*, 32, 1–4, 2005.
- Roberts, N., Brayshaw, D., Kuzucuoglu, C., Perez, R., and Sadori, L.: The mid-Holocene climatic transition in the Mediterranean: Causes and consequences, *The Holocene*, 21, 3–13, 2011a.
- Roberts, N., Eastwood, W. J., Kuzucuoglu, C., Fiorentino, G., and Caracuta, V.: Climatic, vegetation and cultural change in the eastern Mediterranean during the mid-holocene environmental transition, *The Holocene*, 21, 147–162, 2011b.
- Rouis-Zargouni, I., Turon, J.-L., Londeix, L., Essallami, L., Kallel, N., and Sicre, M.-A.: Environmental and climatic changes in the central Mediterranean Sea (Siculo-Tunisian Strait) during the last 30 ka based on dinoflagellate cyst and planktonic foraminifera assemblages, *Palaeogeogr. Palaeoclimatol.*, 285, 17–29, 2010.
- Sadori, L. and Giardini, M.: Charcoal analysis, a method to study vegetation and climate of the Holocene: The case of Lago di Pergusa (Sicily, Italy), *Geobios*, 40, 173–180, 2007.
- Sadori, L. and Narcisi, B.: The Postglacial record of environmental history from Lago di Pergusa, Sicily, *The Holocene*, 11, 655–670, 2001.
- Sadori, L., Zanchetta, G., and Giardini, M.: Last Glacial to Holocene palaeoenvironmental evolution at Lago di Pergusa (Sicily, Southern Italy) as inferred by pollen, microcharcoal, and stable isotopes, *Quaternary Int.*, 181, 4–14, 2008.
- Sadori, L., Jahns, S., and Peyron, O.: Mid-Holocene vegetation history of the central Mediterranean, *The Holocene*, 21, 117–129, 2011.
- Sanchez Goñi, M. F. and Harrison, S. P.: Millennial-scale climate variability and vegetation changes during the Last Glacial: Concepts and terminology, *Quaternary Sci. Rev.*, 29, 2823–2827, doi:10.1016/j.quascirev.2009.11.014, 2010.
- Shakun, J. D., Clark, P. U., He, F., Marcott, S. A., Mix, A. C., Liu, Z., Otto-Bliesner, B., Schmittner, A., and Bard, E.: Global warming preceded by increasing carbon dioxide concentrations during the last deglaciation, *Nature*, 484, 49–54, doi:10.1038/nature10915, 2012.
- Siani, G., Paterne, M., Michel, E., Sulpizio, R., Sbrana, A., Arnold, M., and Haddad, G.: Mediterranean Sea Surface Radiocarbon Reservoir Age Changes Since the Last Glacial Maximum, *Science*, 294, 1917–1920, doi:10.1126/science.1063649, 2001.

- Sicre, M. A., Siani, G., Genty, D., Kallel, N., and Essallami, L.: North-South SST evolution across the central Mediterranean basin during the last deglacial, *Climate of the Past*, in preparation, 2013.
- Stambouli-Essassi, S., Roche, E., and Bouzid, S.: Evolution of vegetation and climatic changes in North-Western Tunisia during the last 40 millennia, *Geo-Eco-Trop*, 31, 171–214, 2007.
- Teller, J. T., Leverington, D. W., and Mann, J. D.: Freshwater outbursts to the oceans from glacial Lake Agassiz and their role in climate change during the last deglaciation, *Quaternary Sci. Rev.*, 21, 879–887, 2002.
- Terral, J.-F., Alonso, N., Capdevila, R. B. i., Chatti, N., Fabre, L., Fiorentino, G., Marinval, P., Jordá, G. P., Pradat, B., Rovira, N., and Alibert, P.: Historical biogeography of olive domestication (*Olea europaea* L.) as revealed by geometrical morphometry applied to biological and archaeological material, *J. Biogeogr.*, 31, 63–77, doi:10.1046/j.0305-0270.2003.01019.x, 2004.
- Tinner, W., van Leeuwen, J. F. N., Colombaroli, D., Vescovi, E., van der Knaap, W. O., Henne, P. D., Pasta, S., D'Angelo, S., and La Mantia, T.: Holocene environmental and climatic changes at Gorgo Basso, a coastal lake in southern Sicily, Italy, *Quaternary Sci. Rev.*, 28, 1498–1510, 2009.
- Tornqvist, T. E. and Hijma, M. P.: Links between early Holocene ice-sheet decay, sea-level rise and abrupt climate change, *Nat. Geosci.*, 5, 601–606, 2012.
- Turon, J.-L.: Le palynoplancton dans l'environnement actuel de l'Atlantique nord-oriental. Evolution climatique et hydrologique depuis le dernier maximum glaciaire, *Mémoires de l'Institut de Géologie du bassin d'Aquitaine*, Université de Bordeaux I, Bordeaux, 313 pp., 1984.
- Tzedakis, P. C.: Seven ambiguities in the Mediterranean palaeoenvironmental narrative, *Quaternary Sci. Rev.*, 26, 2042–2066, 2007.
- Vinther, B. M., Clausen, H. B., Johnsen, S. J., Rasmussen, S. O., Andersen, K. K., Buchardt, S. L., Dahl-Jensen, D., Seierstad, I. K., Siggaard-Andersen, M. L., Steffensen, J. P., Svensson, A., Olsen, J., and Heinemeier, J.: A synchronized dating of three Greenland ice cores throughout the Holocene, *J. Geophys. Res.-Atmos.*, 111, D13102, doi:10.1029/2005JD006921, 2006.
- von Grafenstein, U., Erlenkeuser, H., Brauer, A., Jouzel, J., and Johnsen, S. J.: A Mid-European Decadal Isotope-Climate Record from 15,500 to 5000 Years B.P, *Science*, 284, 1654–1657, doi:10.1126/science.284.5420.1654, 1999.
- Vuorela, I.: Relative pollen rain around cultivated fields, *Acta Botanica Fennica*, 102, 1–27, 1973.
- Walker, M. J. C.: Climatic changes in Europe during the Last Glacial/Interglacial transition, *Quaternary Int.*, 28, 63–76, 1995.
- Watts, W. A., Allen, J. R. M., and Huntley, B.: Vegetation history and palaeoclimate of the Last Glacial period at Lago Grande di Monticchio, southern Italy, *Quaternary Sci. Rev.*, 15, 133–153, 1996.
- Yu, S.-Y., Colman, S. M., Lowell, T. V., Milne, G. A., Fisher, T. G., Breckenridge, A., Boyd, M., and Teller, J. T.: Freshwater Outburst from Lake Superior as a Trigger for the Cold Event 9300 Years Ago, *Science*, 328, 1262–1266, doi:10.1126/science.1187860, 2010.
- Zielhofer, C. and Faust, D.: Mid- and Late Holocene fluvial chronology of Tunisia, *Quaternary Sci. Rev.*, 27, 580–588, doi:10.1016/j.quascirev.2007.11.019, 2008.
- Zielhofer, C., Faust, D., and Linstädter, J.: Late Pleistocene and Holocene alluvial archives in the Southwestern Mediterranean: Changes in fluvial dynamics and past human response, *Quaternary Int.*, 181, 39–54, doi:10.1016/j.quaint.2007.09.016, 2008.